Australian Government
Department of Defence
Defence Science and
Technology Organisation

The Lead Crack Fatigue Lifing Framework

L. Molent[1]*, S.A. Barter*[1] *and R.J.H. Wanhill*[2]

[1]Air Vehicles Division
Defence Science and Technology Organisation

[2]Aerospace Vehicles Division
National Aerospace Laboratory NLR, the Netherlands

DSTO-RR-0353

ABSTRACT

A fatigue lifing framework using a lead crack concept has been developed by the DSTO for metallic primary airframe components. The framework is based on years of detailed inspection and analysis of fatigue cracks in many specimens and airframe components, and is an important additional tool for determining aircraft component fatigue lives in the Royal Australian Air Force (RAAF) fleet. Like the original Damage Tolerance (DT) concept developed by the United States Air Force (USAF), this framework assumes that fatigue cracking begins as soon as an aircraft enters service. However, there are major and fundamental differences. Instead of assuming initial crack sizes and deriving early crack growth behaviour from back-extrapolation of growth data for long cracks, the DSTO framework uses data for real cracks growing from small discontinuities inherent to the material and the production of the component. Furthermore, these data, particularly for lead cracks, are characterized by exponential crack growth behaviour. Because of this common characteristic, the DSTO framework can use lead crack growth data to provide reasonable (i.e. not overly conservative) lower-bound estimates of typical crack growth lives of components, starting from small natural discontinuities and continuing up to crack sizes that just meet the residual strength requirements. Scatter factors based on engineering judgement are then applied to these estimates to determine the maximum allowable service life (safe life limit).

RELEASE LIMITATION

Approved for public release

Published by

Air Vehicles Division
DSTO Defence Science and Technology Organisation
506 Lorimer St
Fishermans Bend, Victoria 3207 Australia

Telephone: (03) 9626 7000
Fax: (03) 9626 7999

© Commonwealth of Australia 2010
AR-014-747
April 2010

APPROVED FOR PUBLIC RELEASE

The Lead Crack Fatigue Lifing Framework

Executive Summary

Many years of quantitative fractography (QF) of fatigue cracking in metallic airframe materials and structures, ranging from coupon to full-scale fatigue tests, and also including components removed from service, have shown that most of the lead cracks grew in an approximately exponential manner. The QF observations covered crack sizes from a few micrometres up to many millimetres and showed that the cracks originated from small discontinuities inherent to the material and production of the component. Furthermore, the lead cracks began to grow shortly - effectively immediately - after the coupons, test articles and service components were subjected to dynamic (fatigue) loading. Based on these observations the DSTO has developed a service component lifing approach called the *lead crack fatigue lifing framework*. This framework has been implemented as an additional tool to determine component fatigue lives for several types of aircraft in the Royal Australian Air Force (RAAF) fleet.

In using a *lead crack concept* the DSTO framework assumes that fatigue cracking begins as soon as an aircraft enters service. This is the same assumption as that made by the original Damage Tolerance (DT) concept developed by the United States Air Force (USAF). However, there are major and fundamental differences. Instead of assuming initial crack sizes and deriving early crack growth behaviour from back-extrapolation of growth data for long cracks, the DSTO framework uses data for real cracks growing from the small inherent discontinuities observed by QF. Furthermore, these data, particularly for lead cracks, are characterized by exponential crack growth behaviour. Because of this common characteristic the DSTO framework can use lead crack growth data to provide reasonable (i.e. not overly conservative) lower-bound estimates of typical crack growth lives of components, starting from small natural discontinuities and continuing up to crack sizes that just meet the residual strength requirements. Scatter factors based on engineering judgement are then applied to these estimates to determine the maximum allowable service life (safe life limit).

This report presents and discusses the lead crack fatigue lifing framework, including its strengths and limitations.

Authors

Loris Molent
Air Vehicles Division

Loris is currently Head, Structural Integrity (Combat and Trainer Aircraft) at the Air Vehicles Division. Loris graduated in 1983 with a Bachelor of Engineering (Aeronautical) from RMIT. Since commencing employment at the then Aeronautical Research Laboratories in 1984, he has worked in the fields of aircraft structural integrity, structural and fatigue testing, advanced bonded repair, aircraft accident investigation and aircraft vulnerability. He has over 200 publications in these technical areas. He has been attached to both the Civil Aviation Department (1985) and the US Navy (NAVAIR, 1990-1991) as an airworthiness engineer. Loris is Head, Structural Integrity Combat and Trainer Aircraft.

Simon Barter
Air Vehicles Division

Simon works as a lead in the Structural Integrity area of the Air Vehicles division. He has a PhD in Engineering Science from Monash University, having achieved undergraduate qualifications in metallurgy, surface finishing and corrosion control from RMIT. During his time at DSTO he has been involved with the metallurgical investigation of aircraft structure and component failures, quantitative fractographic research of cracking in several RAAF aircraft, and the management of full-scale fatigue tests. Additionally he has been involved in the investigation of aircraft oxygen system fires and aircraft accident investigations. He is currently investigating the fatigue and fracture properties of high strength aluminium and titanium alloys.

Russel Wanhill
Aerospace Vehicles Division, NLR, Netherlands

Russell is emeritus Principal Research Scientist in the Aerospace Vehicles Division of the NLR. He has a PhD in Metallurgy from the University of Manchester Institute of Science and Technology and a Doctor of Technical Science degree from Delft University of Technology. He joined the NLR in 1970 and since then has investigated fatigue and fracture of all classes of aerospace alloys, including many service failures. From 1978 to 1996 Russell was head of the Materials Department of the NLR, and in 1979-80 adjunct professor of materials at Delft University of Technology. He is co-author of the book "Fracture Mechanics" (1984), which is now into a second edition, and has written more than 320 NLR reports and publications. In 2002 the Board of the Foundation NLR awarded Russell the first Dr. ir. B.M. Spee Prize for outstanding contributions in the field of aerospace materials. He has recently been working on the analysis of fatigue cracking in GLARE panels from the Airbus 380 MegaLiner Barrel test; and, in collaboration with Simon Barter and Loris Molent, on the use of marker loads for fatigue life assessment and the fatigue crack growth properties of high strength aluminium and titanium alloys. Russell and Simon have also collaborated on a chapter on hydrogen embrittlement for a NATO RTO report, with practical examples from service failures and problems.

Contents

LIST OF SYMBOLS, ABBREVIATIONS AND ACRONYMS

1. INTRODUCTION.......... 1
- **1.1 Fatigue life testing for metallic airframes.......... 1**
- **1.2 Fatigue lifing methods.......... 2**
  - 1.2.1 Royal Australian Air Force (RAAF) lifing criteria.......... 2
  - 1.2.2 Methods of establishing FCG lives.......... 2
- **1.3 USAF DT method [2].......... 3**
- **1.4 DSTO method.......... 4**

2. LEAD CRACKS.......... 5
- **2.1 Lead crack characteristics.......... 5**
- **2.2 Examples of exponential FCG and lead cracks.......... 6**

3. FATIGUE CRACK INITIATION.......... 8
- **3.1 Ideal and realistic (service and production quality) conditions.......... 8**
- **3.2 Fatigue cracking from discontinuities: an example.......... 9**

4. FATIGUE CRACK GROWTH.......... 11
- **4.1 Approximately exponential crack growth.......... 11**
- **4.2 A note about FCG "laws".......... 13**

5. THE LEAD CRACK FATIGUE LIFING FRAMEWORK.......... 13
- **5.1 Framework.......... 13**
- **5.2 Methodology.......... 13**
- **5.3 The Framework Application.......... 14**

6. CONCLUSIONS.......... 17

7. REFERENCES.......... 17

APPENDIX A: EXCEPTIONS TO EXPONENTIAL FCG 21
- **A.1. Introduction 21**
- **A.2. Discontinuity equivalent pre-crack size (EPS) and early FCG 21**
- **A.3. Component thickness and geometry changes 22**
- **A.4. Load shedding 24**
  - A.4.1 Load shedding to adjacent areas and structures 24
  - A.4.2 Load shedding owing to local bending or pin loads .. 25
- **A.5. Residual stresses 26**
- **A.6. FCG retardation due to peak loads 27**
- **A.7. Quasi-static fracture close to final failure 29**
- **A.8. References 30**

APPENDIX B: FATIGUE-INITIATING DISCONTINUITIES 32
- **B.1. Introduction 32**
- **B.2. Examples of discontinuities 33**
  - B.2.1 Poorly finished holes 33
  - B.2.2 Surface treatments 38
  - B.2.3 Porosity 42
  - B.2.4 Constituent particles 43
- **B.3. Fatigue crack initiation in high strength aluminium alloys .. 45**
  - B.3.1 External or internal initiation 45
  - B.3.2 Large constituent particles 46
  - B.3.3 Dispersoids and small constituent particles 47
  - B.3.4 Internal (subsurface) fatigue initiation 49
- **B.4. References 50**

APPENDIX C: LEAD CRACK FCG ESTIMATES 53
- **C.1. Introduction 53**
- **C.2. Example of EPS, a_{RS} and lead crack FCG estimates 54**
- **C.3. Example of lead crack FCG estimates from multiple cracking 55**
- **C.4. References 58**

List of Symbols, Abbreviations and Acronyms

a	crack size
a_0	initial discontinuity or crack size
a_{cr}	critical crack size
a_{RS}	critical crack size at 1.2DLL
AA	aluminium alloy
AFHRS	airframe hours
AVT	Applied Vehicle Technology
BLKHD	bulkhead
β	finite width and crack shape geometry correction factor
CA	constant amplitude
CB	centre barrel (bulkhead)
CCT	centre crack tension
CF	Canadian Forces
CS	central spar
DLL	Design Limit Load
DSTO	Defence Science and Technology Organisation
DT	Damage Tolerance
EPS	equivalent pre-crack size
FALSTAFF	Fighter Aircraft Loading STAndard For Fatigue
FASS	forward auxiliary spar station
FCG	fatigue crack growth
FLEI	fatigue life expended index
FSFT	full-scale fatigue test
GLARE	GLAss REinforced aluminium laminates
IPP	inner pivoting pylon
λ	constant in specific exponential crack growth relations
LHS, RHS	left hand side and right hand side
MLB	MegaLiner Barrel
N	time in specific exponential crack growth relations
NATO	North Atlantic Treaty Organisation
NDI	Non-Destructive Inspection
QF	quantitative fractography
R	stress ratio, S_{min}/S_{max}
RAAF	Royal Australian Air Force
RS	residual strength; also rear spar
RST	residual strength test
RTO	Research and Technology Organisation
S_{max}, S_{min}	maximum and minimum stresses
SF	scatter factor
SFH	simulated flight hours
SLL	safe life limit
t	time
USAF	United States Air Force
VA	variable amplitude

1. Introduction

1.1 Fatigue life testing for metallic airframes

Accurate prediction of the fatigue lives of metallic airframes still presents challenges, particularly for high performance aircraft. There is always a demand for lighter structures with reduced manufacturing and operating costs. This leads to relatively highly stressed and highly efficient designs where fatigue issues can arise at features such as shallow radii at the junction of flanges, webs and stiffeners, as well as at holes and tight radii. As a consequence, there are usually many areas that need to be assessed for their fatigue lives, and many potential locations at which cracking may occur in service.

It is well-known that fatigue is a complex phenomenon that is dependent on many parameters, including the material characteristics (mechanical properties, microstructure and inherent discontinuities, e.g. constituent particles), surface treatments and finishes, the component and structural geometries, dynamic load histories and the environment. Nevertheless, engineering fatigue design relies in-part on baseline coupon tests to assess the many locations identified as susceptible to cracking. The coupons may be loaded by constant amplitude (CA) or representative variable amplitude (VA) load histories, and they may try to represent some feature of a built-up structure. The results of these coupon tests are averaged to give an indication of the life of the structure in a production aircraft. However, there are significant limitations to this approach:

(1) Experience has shown that, in high performance aircraft, the structural components have many features with the potential to crack, and that each of these features is typical of a single type of (more-or-less) representative coupons. Hence, the average indicated life of a component is equivalent to only the shortest average life from tests on several types of coupons.

(2) Even when the most critical feature of a component has been identified and assessed by coupon testing, the coupons are rarely fully representative, notably with respect to the surface treatments and finishes required for production aircraft. This is important because the commencement of fatigue cracking is primarily surface-influenced and therefore greatly dependent on small surface discontinuities inherent to component production, as well as any surface-connected discontinuities inherent to the material.

These limitations are addressed by other means. One way, which is mandatory for all modern aircraft, is to test actual components, part of the structure or even the full airframe, thereby including the effects of component geometry and production. Another way is to improve coupon testing by making the coupons optimally representative of the most fatigue-critical details, e.g. by applying surface treatments and finishes used in component production. This may seem obvious, but it is sometimes neglected or overlooked.

1.2 Fatigue lifing methods

1.2.1 Royal Australian Air Force (RAAF) lifing criteria

The preferred RAAF methodology for lifing aircraft primary structures, e.g. [1], requires establishing the fatigue test life, under representative loading, of a full-scale structure or major component to a residual strength (RS) requirement of 1.2 × Design Limit Load (DLL) without failure. Whether the test structure fails below 1.2DLL or survives, it is necessary to determine the equivalent fatigue life defined by the ability of a structural detail to achieve and survive 1.2DLL with cracking present. In other words, the test time to the critical crack length/depth (a_{RS}) at the RS ≥ 1.2DLL point is required.

For a crack that fails the structure below 1.2DLL the fatigue crack growth (FCG) life is assessed analytically and reduced to a time at which it would have reached the calculated a_{RS} value for a RS = 1.2DLL. For those cracks that survive the RS test load some assessment of the remaining amount of life may be needed. This depends on several factors:

(1) During a complex full-scale fatigue test, it is often necessary to ensure the survival of the test article by removing or modifying cracked locations when the cracks are smaller than the calculated a_{RS} values. These locations become the subject of fleet action prior to the overall life established by the fatigue test, but it may be possible to gain some additional life before the fleet action. This is checked by calculating the remaining FCG life to a_{RS}, thereby establishing a virtual test life (virtual test point) for fleet action.

(2) Although the test may in general establish adequate fatigue lives, it is often not possible to apply representative load histories in all areas. When cracks form at locations in non-representatively loaded areas it may be necessary to calculate the definitive FCG life to a_{RS} and establish additional virtual test points. Such calculations require detailed knowledge of the FCG behaviour under representative and non-representative load histories.

(3) Finally, the load histories experienced by the fleet may turn out to be significantly different to the load histories assumed and applied during testing. As before, such differences may require further analysis of the cracks found during testing, in order to establish new equivalent test lives and virtual test points.

Each of these scenarios needs a framework of rules under which FCG predictions can be made with the aid of data from coupon, component and full-scale fatigue tests. However, before proceeding to this topic, which is the main theme of the present report, methods of establishing the FCG lives are concisely discussed. This is because there is a major and fundamental difference between the method employed in the Damage Tolerance (DT) concept developed by the United States Air Force (USAF) [2] and the currently proposed and used DSTO method.

1.2.2 Methods of establishing FCG lives

Both the USAF DT and DSTO methods assume that defects (cracks, flaws and discontinuities) are already present in new structures, and that these defects must be treated as cracks that are immediately capable of growing by fatigue under service load histories. However, beyond these assumptions there are major and fundamental differences.

1.3 USAF DT method [2]

For critical locations the DT method specifies initial flaw/crack sizes and shapes based on pre-service Non-Destructive Inspection (NDI) capabilities and the assumption that cracks grow soon after the aircraft is introduced into service. The minimum assumed crack dimension is about 0.5 mm, see table 1. Soon after these requirements were introduced, there was some debate about their arbitrariness and unknown conservatism [3]. Subsequently, Lincoln [4] stated that more than ten years of data collection had validated the requirements. However, there is now a consensus that these requirements can lead to predicted FCG lives that are too conservative. This has led to setting up the RTO working group AVT-125 "Future Airframe Lifing Methodologies" within the NATO community, and with which the DSTO confers and participates.

Table 1: USAF MIL-A-83444 safety requirements for assumed initial damage

Types of flaw		*Aspect ratio (a/c)*	*Flaw size a (mm) to be assumed immediately after inspection*		
Description	**Geometry**		**Pre-service inspection with high standard NDI***		**In-service inspection with special NDI***
			Fail-safe	Slow crack growth	
Surface crack#	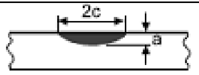	1.0 0.2	1.27	3.18	6.35
Through crack	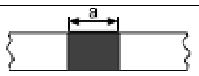		2.54	6.35	12.7
Corner crack at a hole#	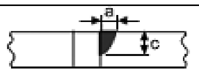	1.0 0.2	0.51	1.27	6.35 mm beyond fastener head or nut
Through crack at a hole	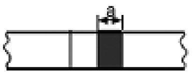		0.51	1.27	6.35 mm beyond fastener head or nut

* NDI = Non-Destructive Inspection
# Definition of *a* used herein.

For continuing damage[1] and non-critical locations the DT method specifies much smaller initial flaw/crack sizes of about 0.127 mm, but allows the aircraft manufacturer to change these requirements if actual initial flaw/crack size information is available - which has rarely been the case until recently [5,6].

Be that as it may, all the specified USAF DT initial flaw/crack sizes are questionable or arbitrary assumptions. For continuing damage and non-critical locations the predicted early FCG behaviour is also questionable since it is derived from back-extrapolation of (a) VA long crack growth data or (b) VA growth curves derived from long crack CA data, with both methods using analytical models "tuned" to long crack growth behaviour. These issues of initial flaw size and VA crack growth determination from CA, together with potentially overly-conservative predictions of FCG lives for critical locations, constitute significant limitations to the DT method.

---

[1] This relates to built-up components where, for example, a crack from one side of a hole grows to a free-edge and results in crack initiation or acceleration of an existing crack from the other edge of the hole or another location in the component [2].

1.4 DSTO method

The DSTO method has been developed from many years of detailed quantitative fractography (QF) of fatigue cracking in metallic airframe materials and structures, ranging from coupon to full-scale fatigue tests, and also including components removed from service. The QF observations covered crack sizes from a few micrometres up to many millimetres and showed that the cracks originated from small discontinuities inherent to the material and component production. These discontinuities are discussed in Section 3 of this report.

For high performance aircraft the detailed QF observations were–and are–essential to determine the FCG rates, particularly where most of the life of a fatigue crack is spent as a relatively small crack. QF data make it possible to (a) characterise the crack-generating discontinuities and their populations, (b) account for variability in small crack FCG behaviour, a notorious problem that is difficult or impossible to tackle in any other way, and (c) predict total lives from larger or smaller discontinuities. All of this information can be used to make more accurate predictions of FCG lives in service. Furthermore, a key point is that the *lead cracks* began to grow shortly–effectively immediately–after the test coupons, components, full-scale structures and service components are subjected to fatigue loading.

Based on these observations, and applying a *lead crack concept* which assumes that lead cracks in production quality aircraft components and structures immediately begin to grow under service load histories, the DSTO has developed a service component lifing approach based on the *lead crack fatigue lifing framework*. Under (or using) this framework a methodology has been implemented as an additional tool to determine component fatigue lives for several types of aircraft in the Royal Australian Air Force (RAAF) fleet.

This report presents the framework, with examples from test programmes used in lifing RAAF aircraft. Examples of typical crack growth behaviour, and departures from it, are also presented.

2. Lead Cracks

If a particular region of a structure has the propensity to crack, it is possible that a number of cracks will nucleate and grow. The crack that grows fastest in this region is the lead crack. Since there will probably be a number of regions across an entire structure that will crack, there will most likely be a number of lead cracks across the entire structure and one of these will ultimately cause the failure of the structure.

Many observations at the DSTO e.g. [7-10] and by other researchers, e.g. [11-13], have shown that approximately exponential FCG is a common occurrence for naturally-initiating *lead* cracks (i.e. those leading to first failure) in test specimens, components and airframe structures subjected to VA load histories. At this point, it is important to note that the lead cracks come from a typical population of cracks. They are not cracks growing from the rare and exceptional discontinuities classed as "rogue flaws".

2.1 Lead crack characteristics

The lead cracks have the following general characteristics:

(1) They start to grow shortly after testing begins or the aircraft is introduced into service.

(2) Subject to several conditions (see below) they grow approximately exponentially with time, i.e. FCG may be represented by an equation of the form $a = a_0e^{\lambda N}$, where a is the crack size at time N, a_0 is the initial crack size and λ is a constant that includes the geometrical factor β, see point (3) below. The conditions are:

   (a) Little error is made when assessing the effective crack size (EPS) of the fatigue-initiating discontinuity. An underestimate will cause a small temporary departure from an exponential trend near the commencement of FCG.

   (b) The crack does not grow into an area with a significant thickness change, particularly if the crack length/depth is small compared to the specimen or component thicknesses or widths.

   (c) The crack is not unloaded, either (i) by the cracked area losing stiffness and shedding load to other areas of the specimen, component or structure; or because it grows (ii) towards a neutral axis due to bending loads or (iii) away from an externally induced stress concentration such as a pin-loaded hole in a multi-pin loaded joint.

   (d) The crack does not encounter a significantly changing stress field by growing into or from an area containing residual stresses.

   (e) FCG is not retarded by infrequent very high loads (usually in excess of 1.2 x the peak load in the load history).

   (f) The small fraction of FCG life influenced by quasi-static fracture close to final failure is ignored.

These conditions for approximately exponential FCG are discussed further in Appendix A. Within the bounds of these conditions, the DSTO's observations of the formation, growth and failure of lead cracks have led to the following deductions:

(3) The usually important geometrical factor β (which depends on the ratios of the crack length and shape to the width and thickness of the specimen or component) does not appear to influence the FCG as much as might be expected. For low K_t features the majority of the life is spent when the crack is physically small, so β does not change much. However, even when a crack initiates at an open hole and the calculated β changes rapidly, the lead cracks still appear to grow exponentially. (This is not to say there is no geometry influence. For example, under the same net section stresses, FCG from open holes accelerates more than from low K_t details.)

The reason or reasons for the small influence of β requires further research.

(4) Typical initial discontinuity sizes are about equivalent to a 0.01 mm deep fatigue crack, see for example [6,8]. In other words, a 0.01 mm deep crack is a good starting point (or Equivalent Pre-crack Size - EPS) for FCG assessment. N.B: this EPS is well below the smallest initial flaw/crack size to be assumed in the USAF DT method, see subsection 1.2.2.

(5) Cracks may also grow exponentially within residual stress fields, although the exponent will be influenced by these stress fields, see for example [14,15].

(6) If (very) high loads occur periodically in the load history, then the average FCG may still have an exponential trend [7].

(7) The metallic materials used in highly stressed areas of high performance aircraft have typical critical crack depths[2] of about 10 mm, see for example [6,8].

2.2 Examples of exponential FCG and lead cracks

Exponential FCG from typical small discontinuities occurs in several materials, irrespective of load histories [7] (e.g. tension- or compression-dominated, and manoeuvre or gust spectra), aircraft type [8] and structural geometry [9,16]; and for fatigue crack sizes from a few micrometres to many millimetres.

Figure 1 gives examples of exponential FCG curves extending over 2−3 orders of magnitude in crack size. The data were obtained from QF measurements on samples cut from the lower skin of an F-111 wing removed from service and tested under flight-by-flight block loading [17]. The FCG rates (gradients of the FCG curves) were mostly similar, even though the cracks occurred at numerous span-wise and chord-wise locations and covered two-thirds of the wingspan. This means that despite variations in geometrical details and locations, similar FCG rates pertain under similar loading conditions. This trend has been observed for other aircraft structures [8].

---

[2] Although final failure of many highly stressed components may be at larger crack sizes, it is usually found that significant quasi-static fracture preceded failure. This observed behaviour is rarely accounted for by standard laboratory tests. See Chapter 8 in [5] for a particularly illustrative example.

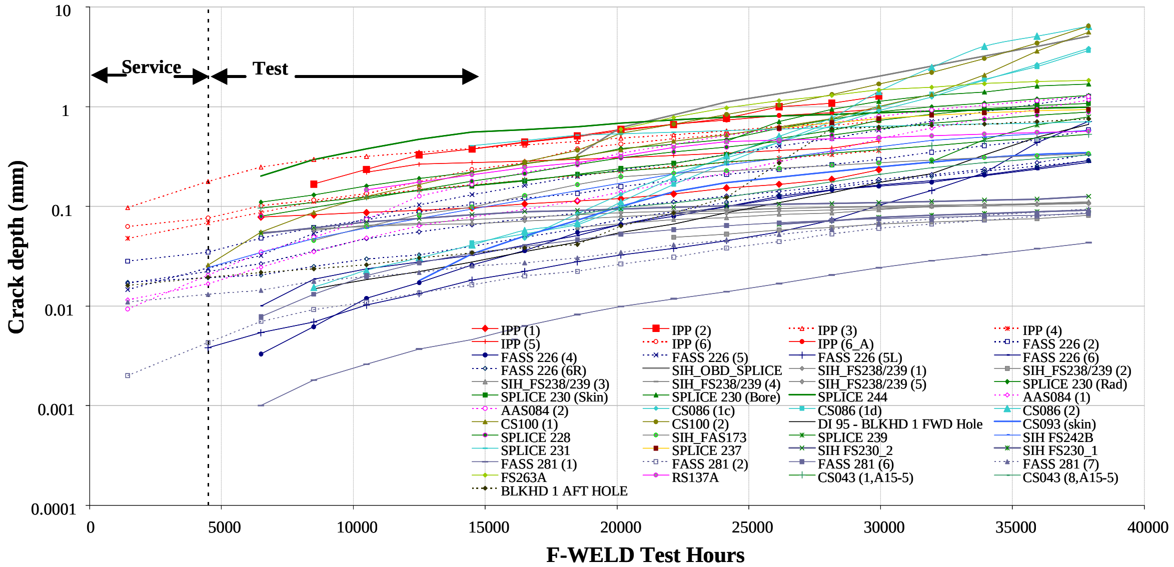

Figure 1: Sample of FCG curves from different locations in the aluminium alloy (AA) 2024-T851 lower wing skin of an F-111 test article removed from service [17]. CS = central spar, BLKHD = bulkhead, FASS = Forward Auxiliary Spar Station inches, IPP = Inner Pivoting Pylon, RS = Rear Spar.

Besides clearly demonstrating exponential FCG behaviour and similar FCG rates, this log crack size *versus* linear life plot has a couple of additional advantages:

- The FCG behaviours of small cracks are more clearly seen than on a double-linear plot.
- Given mostly similar FCG rates it is seen that the major source of scatter (for the same loading) is the initial discontinuity/crack size. This demonstrates the importance of obtaining good estimates of EPS values.

From the example in Figure 1 and the attendant discussion it may be seen that simplified but reasonably accurate FCG life estimates can be derived as follows:

- Assume immediate in-service exponential FCG from initial discontinuities.
- Select several locations and areas.
- Choose a number of initial discontinuity/crack sizes (EPS) and final crack sizes characteristic of these locations and areas.
- Choose characteristic exponent values (or possibly one overall value if the FCG rates are similar) in combination with initial discontinuity sizes and final crack sizes to estimate FCG lives for these locations and areas.

Comparison of these estimates will enable determining the lead crack at any given life and its location. For example, Figure 1 shows that at 20,000 test hours the lead crack was at SPLICE 244, but at 35,000 test hours the lead crack was at CS086. The reasons for this change are (a) the larger initial crack depth for the SPLICE 244 location and (b) the higher crack growth rates for the crack at the CS086 location, whereby this crack overtook the SPLICE 244 crack at about 28,000 test hours.

3. Fatigue Crack Initiation[3]

3.1 Ideal and realistic (service and production quality) conditions

Under more or less ideal conditions, typically for carefully prepared specimens[4] tested in laboratory air, a significant period of fatigue-induced microstructural damage can precede fatigue crack initiation. This may also be the case for highly finished engine components and low-stressed parts in secondary structures and helicopters, although service conditions can allow other mechanisms like corrosion, fretting and incidental damage to contribute to the pre-crack damage.

In contrast, production aircraft components and structures often have many sources of surface or near-surface discontinuities capable of initiating fatigue cracking. These include various forms of machining damage (scratches, grooves, burrs, small tears and nicks); etch pits from surface treatments (pickling, anodising); porosity, especially in thick aluminium alloy plate and castings; and in the case of aluminium alloys and steels, constituent particles that may themselves be cracked. Titanium alloys are a special case, but they too can have material discontinuities, though very rarely [18].

Figure 2 shows some examples of discontinuities, illustrating their variety. More are given in Appendix B, which also includes a concise review of fatigue crack initiation in aluminium alloy components and structures, since these materials are the most widely used in metallic airframes.

Although the discontinuities are mostly small – of the order of 0.01 mm in depth [6,8] — they can initiate fatigue cracking quickly in highly stressed specimens, components and structures. This has been shown by DSTO studies [6-8,10,19,20] and others [21,22], and an example is given in subsection 3.2. Furthermore, structures with many critical features, e.g. bolt holes, or large areas under high stress, are susceptible to multiple crack initiation. One or more of these cracks will lead the others to become the critical cracks that determine the FCG life.

---

[3] The title of this Section is somewhat contentious. The eminent researcher, D.W. Hoeppner, prefers "nucleation" to "initiation", which he regards as misleading. This is because the terms "fatigue crack initiation" and "life to first crack" have often been used imprecisely, without regard to the physical process or processes that preceded crack formation.

[4] The specimens may be precision machined finished and then highly polished.

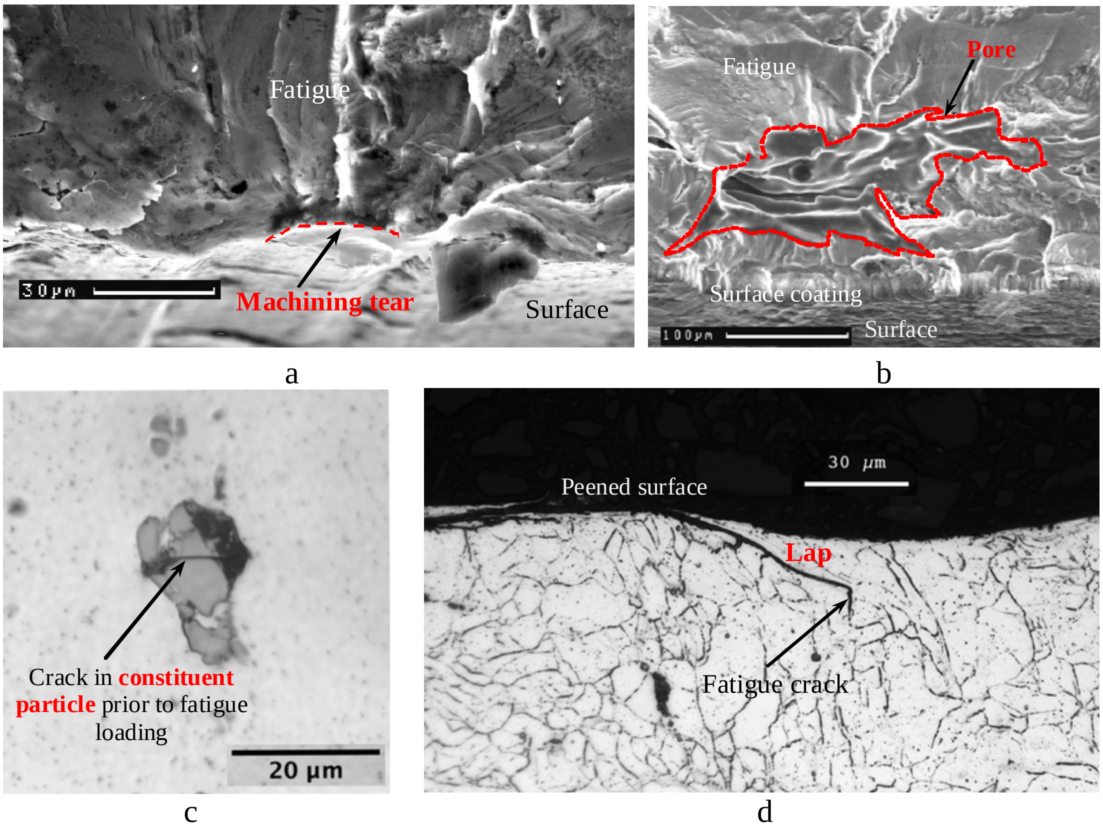
Fatigue
30µm
Machining tear
Surface
a
Fatigue
Pore
Surface coating
100µm
Surface
b
Crack in constituent particle prior to fatigue loading
20 µm
c
30 µm
Peened surface
Lap
Fatigue crack
d

Figure 2: *Some examples of discontinuities that can exist in a metallic airframe at the time it enters service. Each discontinuity will act, or has acted, as an effective crack starter, reducing fatigue crack formation to a few effective load cycles.*

3.2 Fatigue cracking from discontinuities: an example

As mentioned in subsection 3.1, small discontinuities can cause fatigue cracking very quickly at high stress levels. It was also mentioned in subsection 1.1 that the initiation of fatigue cracking is primarily from surface discontinuities.

To illustrate these points and their interrelation, Figure 3 shows QF data for flight simulation FCG from surface-connected and (slightly) subsurface discontinuities in highly stressed aluminium alloy specimens. Most of the FCG-initiating discontinuities were smaller than 0.05 mm and crack growth began effectively immediately when they were surface-connected. However, for specimens KS1G3 and KS1G66 the FCG-initiating discontinuities were subsurface and there were apparent delays of 10,000 and 26,000 flight blocks before crack growth began. The reason for these apparent delays is that subsurface crack growth would have occurred *in vacuo* at much slower rates than in air [23]. Once the cracks contacted the surface (and thus the environment) their FCG rates became similar to those for other specimens tested at the same stress levels.

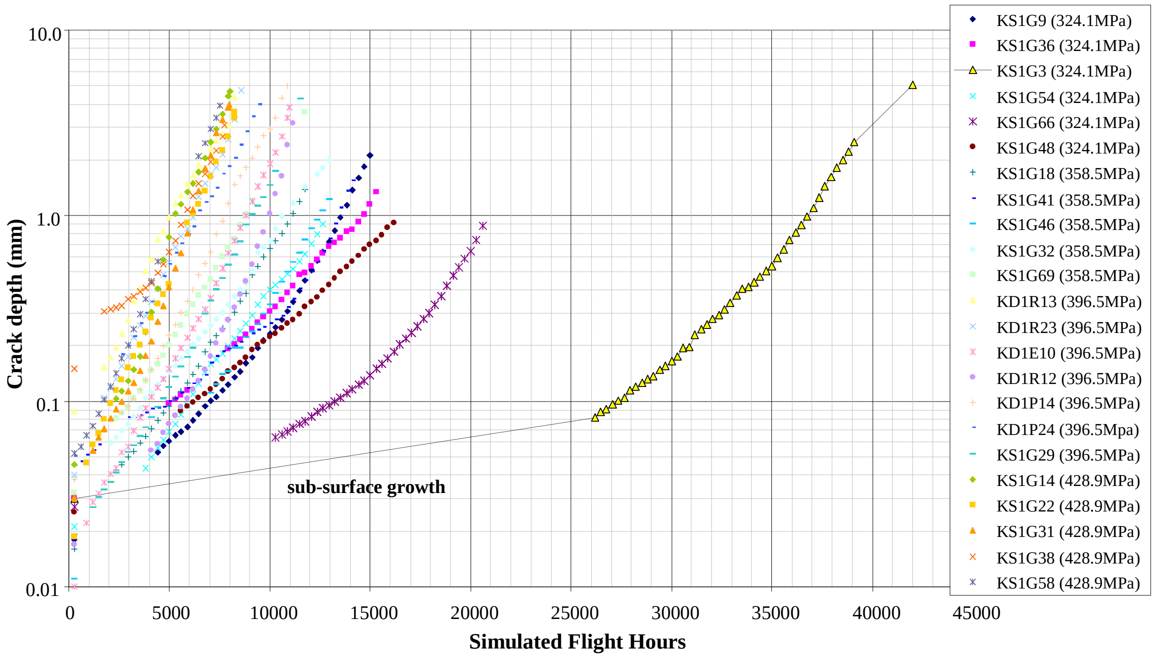

Figure 3: FCG data for highly stressed AA7050-T7451 aluminium alloy specimens tested under combat aircraft flight-by-flight block loading at four stress levels. One block represents about 300 airframe hours (AFHRS) and each data point represents the crack growth increment per block.

Subsurface fatigue crack initiation is considered highly exceptional in aircraft components and structures unless they have undergone surface treatments, e.g. shot peening, to enhance the fatigue resistance. Although such treatments are not relied upon during design for fatigue lifing purposes, shot peening is a favoured remedial action for areas found to have insufficient life. An example is given in Appendix A. The behaviour of subsurface-initiated fatigue cracks is discussed in more detail in Appendix B.

4. Fatigue Crack Growth

4.1 Approximately exponential crack growth

As mentioned in Section **2**, many observations have shown that approximately exponential FCG commonly occurs for naturally-initiating lead cracks. In fact, the observation of exponential FCG has a long history, going back to the 1950s [24]. This behaviour is described by the following simple relationships:

$$a = a_0 e^{\lambda N} \qquad (1)$$

$$\ell n(a) = \lambda N + \ell n(a_0) \qquad (2)$$

These relationships mean that the FCG data appear to be well represented by straight lines on plots of ℓn (log) crack size *versus* life and ℓn (log) FCG rate *versus* ℓn (log) crack size. Figures 1 and 3 are examples of the first type of plot, and Figure 4 is an example of the second type.

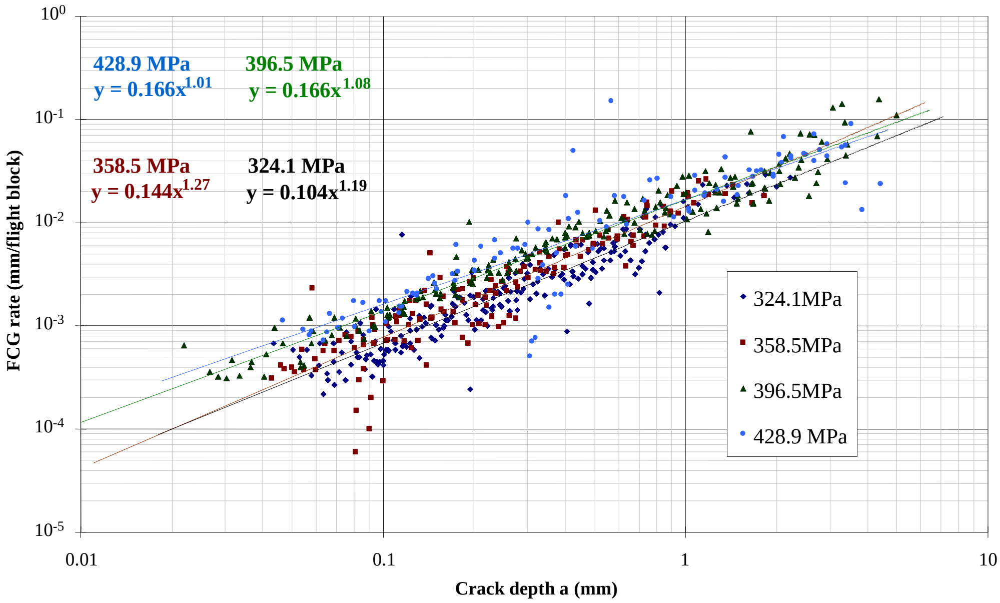

Figure 4: FCG rate data from Figure 3

Several points are to be noted about the example in Figure 4:

(1) The stress level dependence in Figure 3 is reflected in Figure 4.

(2) Trend lines for each set of stress level data have slopes reasonably close to 1 *over 3 orders of magnitude* for both the FCG rates and crack depths. This means that there is a wide range in which the FCG rates are approximately proportional to the crack depths and hence indicate approximately exponential FCG. The wide range of this approximation is a robust affirmation of its applicability and usefulness.

(3) There is data scatter with occasional outliers. Some of the scatter may come from QF measurement difficulties, but local material differences can also play a role, especially when the cracks are small and extend through only a few grains [25]. This point is

illustrated by Figure 5, which is a fractograph for a small fatigue crack in a large-grained aluminium alloy. The fractograph shows significant local variability in the FCG rate for a block of CA R = 0.7 cycles applied between blocks of 5000 CA R = 0.1 cycles, all with the same maximum load.

N.B: although differentiation to obtain Figure 4 reveals data scatter, comparison with Figure 3 shows that the log crack size *versus* linear life plots for each crack are stable**.** This is a common observation, see for example Figures 6 and 16 in [26]. Differentiation to obtain FCG rates accentuates quite small differences in the progression of crack growth. This can be useful for detailed analyses of crack growth but is not relevant to the DSTO lead crack lifing method, which uses log crack size *versus* linear life plots.

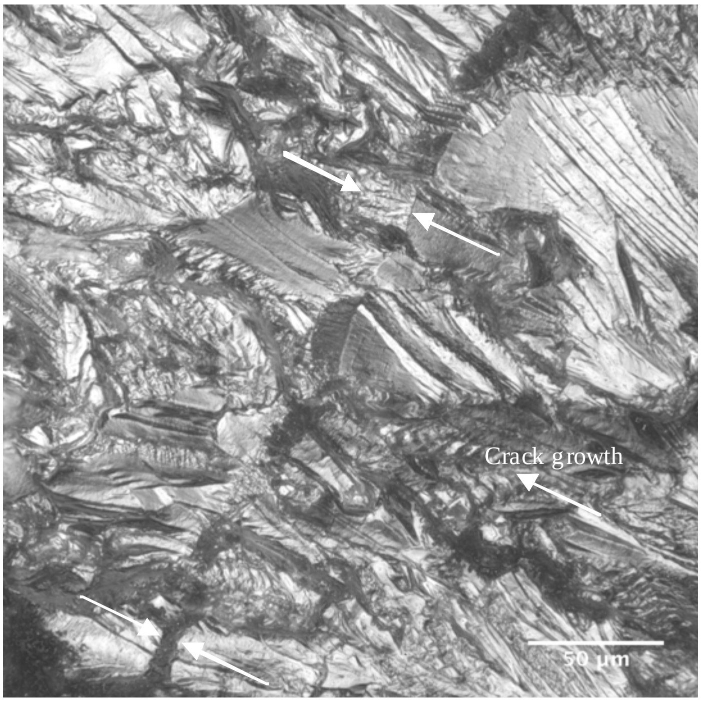

Figure 5: An example of material-related FCG rate variability from the fracture surface of an AA7050-T7451 aluminium alloy specimen at about 1mm in depth. The band from lower left to top right was formed by a block of CA R = 0.7 cycles applied between blocks of 5000 CA R = 0.1 cycles, all with the same maximum load. Note the width variation of the band at the two arrowed positions.

4.2 A note about FCG "laws"

The approximately exponential FCG behaviour of lead cracks under VA load histories is not a "law" but an empirical relationship, albeit a well-established one. There are *no* FCG "laws", although many empirical relationships are referred to as such. This was pointed out more than 30 years ago by D.W. Hoeppner and W.E. Krupp [27], who listed some 33 "laws". However, the proliferation of FCG "laws" continues and there are now at least 186 [28].

Most of the "laws" refer only to CA loading, often using the very well-known Paris "law" [29] as a starting point. Also, none do more than implicitly include chemical and environmental effects, which have significant influences on FCG, e.g. [31-33], especially under VA loading [34-37].

In short, given the appropriate circumstances one crack growth "law" is as good as, or better than, any other. This pragmatic view prompts our assertion of the usefulness and applicability of the approximately exponential FCG behaviour of lead cracks in aircraft components and structures initiated from typical manufacturing discontinuities.

5. The Lead Crack Fatigue Lifing Framework

5.1 Framework

The lead crack fatigue lifing concept has been developed on a framework of observations to calculate virtual test points from full-scale and large component tests, unanticipated service cracking, and sometimes from cracking in representative coupons. The key elements of the framework are (see subsection 2.1):

(1) Lead cracks start to grow shortly after testing begins or the aircraft is introduced into service and subjected to flight loads;

(2) Lead cracks start growing from material production discontinuities;

(3) Lead cracks grow *approximately* exponentially with time; and

(4) The small fraction of FCG life influenced by quasi-static fracture close to final failure is insignificant.

5.2 Methodology

Referring to Figure 1 in Section 2 we gave a step-by-step procedure for determining the lead crack at any given life and location and subsequently calculating its safe life. The procedure, based on the framework described above, contains the following elements:

(a) The assumption of immediate in-service exponential FCG from initial material discontinuities;

(b) An accurate measure of the initial discontinuity and crack sizes, in the form of an EPS for the locations and areas to be assessed;

(c) An accurate measure of the final crack size characteristics (at end of cycling or failure) for the locations and areas to be assessed;

(d) A measure of the characteristic exponents of FCG from the EPSs for the lead crack of the locations of interest;

(e) An estimate of the FCG lives of the lead cracks which becomes an estimate of the virtual test points for each location and area;

(f) The pooling of the estimated lives for each location within each area to calculate the average life of the location; and

(g) The application of an appropriate SF to the average life to determine the safe life of the location.

This procedure is a general one. It is feasible and straightforward if there are numerous FCG data from a fully representative full-scale fatigue test. This may not be the case, for several reasons:

(1) An obvious reason is that QF FCG data may be unavailable or unobtainable. These data would have to be acquired from separate programmes of coupon and component testing.

(2) Structural modifications to ensure the survival of the test article result in uncertainties as to the service lives in the modified locations and areas.

(3) The test load history may be unrepresentative in some locations and areas owing to test rig/structural assembly limitations and differing load histories in service.

(4) Unanticipated service cracking problems, i.e. premature cracking and cracks in locations and areas deemed to have been non-critical during prior analysis and testing.

Reasons (2) and (3) have already been mentioned when discussing the RAAF lifing criteria in subsection 1.2.1. Reasons (2) − (4) require re-assessment of the FCG lives and establishment of new and additional virtual test points for fleet action. These reasons and their accompanying scenarios need a framework of rules for obtaining reliably conservative predictions of FCG lives. The application of the framework is set out in subsection 5.3.

The details of using the methodology are often complex, since it may be necessary to assess and provide robust and comparable lead crack FCG data from different sources [38]. Appendix C gives examples: one is fairly straightforward, subsection C.2, while the other is more complex, subsection C.3. These examples are referred to within subsection 5.3.

5.3 The Framework Application

The application of the framework may be set out in several steps:

(1) Choice of initial discontinuity and crack sizes characteristic of the locations and areas to be assessed. Characteristic discontinuities can be converted to equivalent pre-crack sizes (EPS) using a well-established empirical expression due to Murakami and Endo [37].

If there is no information on initial discontinuities, e.g. when a crack has been blended out during a full-scale fatigue test, then EPS estimates may be possible by back-extrapolating FCG data for cracks in the same area or location. An example is included in subsection C.2.

(2) Choice of final crack sizes characteristic of the locations and areas to be assessed. These crack sizes are preferably the a_{RS} values demonstrated from the RS requirement of 1.2DLL. Or else the critical crack sizes $a_{cr} \equiv a_{RS}$, when further crack growth would have been rapid and structural repairs or modifications were made: an example is included in subsection C.2. Alternatively, the a_{RS} values can be obtained analytically.

(3) Choice of characteristic exponents for fatigue crack growth from the EPS. This step must provide reliably conservative estimates of FCG lives. Hence, much care is needed in deriving and choosing the exponents. The optimum situation is when QF data includes early crack growth from the initial discontinuities. This is not always possible, obviously in the case where a crack has been blended out, or if QF cannot analyse early FCG for a particular load history.

However, the crack sizes at fatigue test end-points and in components retired from service can be used with the EPS to make first estimates of the exponents. These estimates can be adjusted using FCG data from QF-amenable test load histories applied to (a) similar cracks in test coupons or components and (b) *the same* cracks in retired components.

(4) Combine the previous steps, together with the assumption of immediate in-service fatigue crack growth, to estimate the FCG lives of the lead cracks and their virtual test points for each location and area. Examples are given in subsections C.2 and C.3.

(5) Pool the estimates for each location within each area. This step requires that FCG data and crack growth plots obtained under different circumstances, notably under different load histories, be converted to a common fatigue life timeframe. For the F/A-18 in RAAF service, from which the example data in Figure 6 has been drawn, this timeframe is the fatigue life expended index (FLEI), which is the estimated *equivalent* service hours at which an aircraft has accumulated the same damage as the F/A-18 fatigue test article known as FT55 (the results of an earlier test, ST16, are also included in this example to increase its conservatism), divided by the SF, where SF is a scatter factor based on engineering experience[5].

Further explanation of the relation between the FLEI and design target life of the airframe (AFHRS) is necessary here. The full-scale structure or major components are required to meet RS = 1.2DLL, see subsection 1.2.1, at a fatigue test life of (SF X AFHRS) *equivalent* hours. If this is achieved, the safe life limit (SLL) of any aircraft is reached when the FLEI = 1. For the examples given in Figure 6 and Appendix C, the design target life AFHRS is 6000 hours and the scatter factor is 2.8, so that the required *equivalent* number of full-scale test hours was 16,800. The safe life limit of any aircraft is then reached when the FLEI = 1 = 6000 *equivalent* hours[6].

This rather involved procedure is necessary because individual aircraft will experience differing service load histories, such that a common fatigue life timeframe—the FLEI—must be used to assess the fatigue life expenditure of the fleet. As mentioned above, this common fatigue life timeframe is also required for pooling the lead crack FCG estimates. It should be noted that the in-service calculated FLEI of an individual aircraft is designed to be suitably conservative[7] (see Figure 6).

---

[5] Engineering experience, as far as the appropriate selection of a SF is concerned is codified in various standards. In the case of the F/A-18, in RAAF service, Def-Stan-970 is the reference document.

[6] That the average FLEI = 1.0 in the example provided in Figure 6 was purely fortuitous.

(6) From the pooled estimates of virtual test points calculate the logarithmic average of the FLEI values at the critical crack sizes a_{RS} (or $a_{cr} \equiv a_{RS}$). Divide this average by the scatter factor SF to obtain the new (or re-assessed) safe life limits (SLL) for each area. Figure 6 gives an example for the web of a fuselage bulkhead in a F/A-18 Hornet aircraft [38]. The minimum web thickness, 4.32 mm, was conservatively chosen to be the critical crack depth $a_{cr} \equiv a_{RS}$. Note that the re-assessed SLL lies below all the virtual test points, i.e. it is conservative.

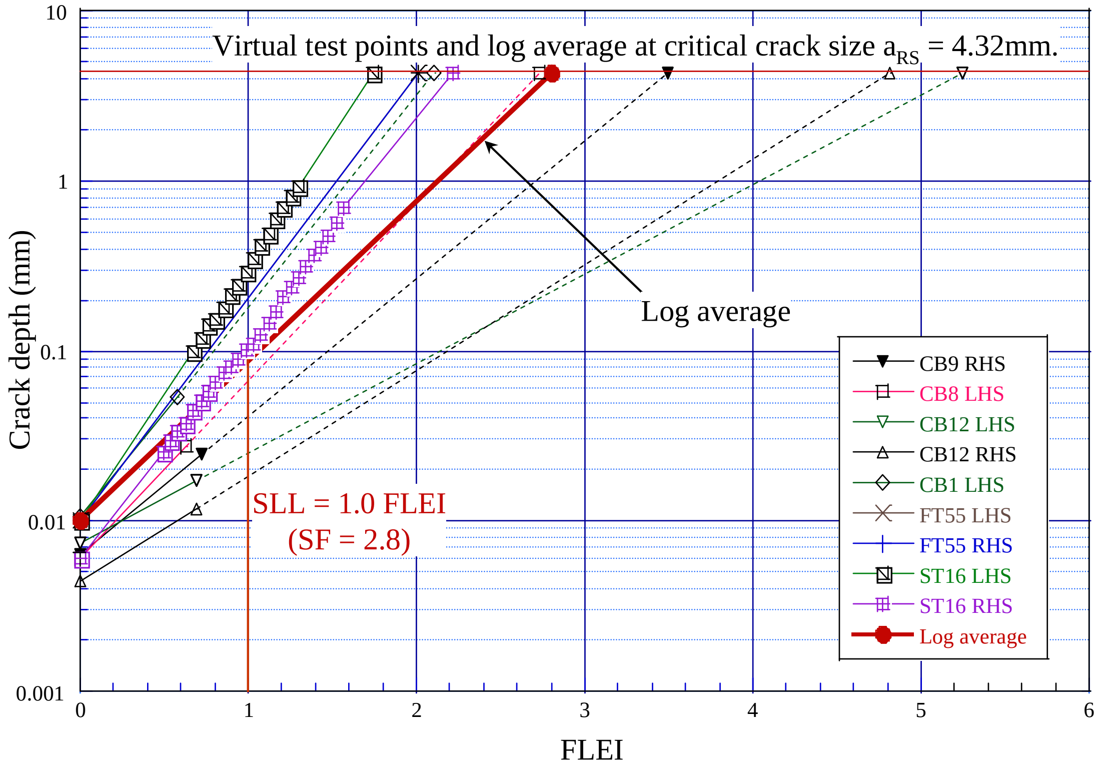

Figure 6: Pooled estimates of exponential FCG for several lead cracks, their virtual test points, the logarithmic average of these virtual test points, and the re-assessed SLL for the web of a fuselage bulkhead in a combat aircraft, using an experience-based scatter factor (SF) of 2.8 [38]. FT55 & ST16 = Full Scale Fatigue Test; CBxx = in-service aircraft. Crack depths at zero SFH = EPS; crack depths at approximately 4000 SFH = measured in-service crack depth from tear-down; dashed lines are extrapolations to the web thickness.

---

[7] In the case of the F/A-18, from which the example in Figure 6 is taken, the RAAF FLEI-based tracking system (MSMP2) has been shown to give a good comparison of the damage accumulated by aircraft when compared to FT55 damage. The comparison of spectra, which included the most benign and severest spectra taken from service aircraft, gave acceptable variability and damage estimates that were generally conservative with respect to the common FT55 baseline spectrum. However, this may not be true for other aircraft types or other methods of tracking. This tracking variability needs to be considered on a case-by-case basis, and any further scatter that this variability imposes needs to be added to the SF that is ultimately used.

Each step of this framework requires careful and expert consideration, as the examples in Appendix C show. The final step, exemplified by Figure 6, is considered to provide a reasonable and reliably conservative estimate of the SLL.

6. Conclusions

This report has presented a lead crack fatigue lifing framework and methodology for metallic primary airframe components. The framework is based on many years of detailed inspection and analysis of fatigue cracks in airframe materials and structures, ranging from coupon to full-scale fatigue tests and also including components removed from service. This framework and its exploitation provide an important additional tool for determining aircraft component fatigue lives in the RAAF fleet.

7. References

[1] Royal Australian Air Force, Structural Analysis Methodology – F/A-18A/B, ASI/2006/1114755 Pt1 (18), Issue 2, AL2, 7 December 2007.

[2] Military Specification Airplane Damage Tolerance Requirements, MIL-A-83444 (USAF) 1974.

[3] Broek, D. Damage tolerance in practice, Lecture 11 in: Fracture Mechanics Design Methodology, AGARD Lecture Series No. 97, Advisory Group for Aerospace Research and Development, Neuilly-sur-Seine, France, 1978.

[4] Lincoln, J.W. Damage tolerance - USAF experience. Durability and Damage Tolerance in Aircraft Design. Proceedings of the 13th Symposium of the International Committee on Aeronautical Fatigue (editors A. Salvetti and G. Cavallini), Engineering Materials Advisory Services Ltd., Cradley Heath, West Midlands, UK, pp. 265-295, 1985.

[5] Wanhill, R.J.H. Damage tolerance engineering property evaluations of aerospace aluminium alloys with emphasis on fatigue crack growth, NLR Technical Publication TP 94177, National Aerospace Laboratory NLR, Amsterdam, the Netherlands, 1995.

[6] Molent, L., Sun, Q. and Green, A.J. Characterisation of equivalent initial flaw sizes in 7050 aluminium alloy. *Fatigue and Fracture of Engineering Materials and Structures*, Vol. 29, pp. 916-937, 2006.

[7] Barter, S., Molent, L., Goldsmith, N. and Jones, R. An experimental evaluation of fatigue crack growth. *Engineering Failure Analysis*, Vol. 12, pp. 99-128, 2005.

[8] Molent, L. and Barter, S. A. A comparison of crack growth behaviour in several full-scale airframe fatigue tests, *International Journal of Fatigue*, Vol. 29, pp. 1090-1099, 2007.

[9] Jones, R., Molent, L. and Pitt, S. Understanding crack growth in fuselage lap joints. *Theoretical and Applied Fracture Mechanics*, Vol. 49, pp. 38-50, 2008.

[10] Molent, L., Singh, R. and Woolsey, J. A method for evaluation of in-service fatigue cracks, *Engineering Failure Analysis*, Vol. 12, pp. 13-24, 2005.

[11] Underhill, P.R. and DuQuesnay, D.L. The effect of dynamic loading on the fatigue scatter factor for Al 7050, *International Journal of Fatigue*, Vol. 30, pp. 614–622, 2008.

[12] Liao, M., Benak, T., Renaud, G., Yanishevsky, M., Bellinger, N., Mills, T., Prost-Domasky, S. and Honeycutt K. The development of short/small crack model for airframe materials. 11th Joint NASA/FAA/DOD Conference on Aging Aircraft, Phoenix, Arizona, USA, 21-24 April 2008.

[13] Mohanty, J.R., Verma, B.B. and Ray, P.K. Prediction of fatigue life with interspersed mode-I and mixed-mode (I and II) overloads by an exponential model: extensions and improvements, *Engineering Fracture Mechanics*, Vol. 76, pp. 454-468, 2009.

[14] Barter, S. A. Fatigue crack growth in 7050T7451 aluminium alloy thick section plate with a glass bead peened surface simulating some regions of the F/A-18 structure, DSTO-TR-1477, Defence Science and Technology Organisation, Melbourne, Australia, 2003.

[15] Walker, K., Weller, S. and Walker, J. F-111 wing pivot fitting upper plate critical features fatigue assessment - pre wing optimisation modification, DSTO-TR-1682, Defence Science and Technology Organisation, Melbourne, Australia, 2005.

[16] Huynh, J., Molent, L. and Barter, S. Experimentally derived crack growth models for different stress concentration factors, *International Journal of Fatigue*, Vol. 30, pp. 1766-1786, 2008.

[17] Boykett, R., Walker, K. and Molent, L. Sole operator support for the RAAF F-111 fleet. 11th Joint NASA/FAA/DOD Conference on Aging Aircraft, Phoenix, Arizona, USA, 21-24 April 2008.

[18] Wanhill, R.J.H. and Barter, S.A. Fatigue of β processed and β heat-treated titanium alloys: A contribution to the DSTO - NLR joint programme of Damage Tolerance and Durability assessment of beta annealed Ti-6Al-4V plate, NLR Technical Publication NLR-TP-2009-036, National Aerospace Laboratory NLR, Amsterdam, the Netherlands, 2009.

[19] Zhuang, W., Barter, S. and Molent, L. Flight-by-flight fatigue crack growth assessment, *International Journal of Fatigue*, Vol. 29, pp. 1647-1657, 2007.

[20] Molent, L. Fatigue crack growth from flaws in combat aircraft, *International Journal of Fatigue*, Vol. 32, pp. 639-649, 2010.

[21] Murakami, Y. and Miller, K.J. What is fatigue damage? A viewpoint from the observation of low cycle fatigue process, *International Journal of Fatigue*, Vol. 27, pp. 991-1005, 2005.

[22] Payne, J., Welsh, G., Christ, Jr., R.J., Nardiello, J. and Papazian, J.M. Observations of fatigue crack initiation in 7075-T651, *International Journal of Fatigue*, Vol. 32, pp. 247-255, 2010.

[23] Wanhill, R.J.H. Fractography of fatigue crack propagation in 2024-T3 and 7075-T6 aluminum alloys in air and vacuum, *Metallurgical Transactions A*, Vol. 6A, pp. 1587-1596, 1975.

[24] Frost, N.E. and Dugdale, D.S. The propagation of fatigue cracks in test specimens, *Journal of Mechanics and Physics of Solids*, Vol. 6, pp. 92-110, 1958.

[25] McClung, R.C., Chan, K.S., Hudak, Jr., S.J. and Davidson, D.L. Behavior of small fatigue cracks, *ASM Handbook Volume 19 Fatigue and Fracture*, (editors S.R. Lampman *et al.*), ASM International, Materials Park, Ohio, USA, pp. 153-158, 1996.

[26] Wanhill, R.J.H. and Hattenberg, T. Fractography-based estimation of fatigue crack "initiation" and growth lives in aircraft components, NLR Technical Publication NLR-TP-2006-184, National Aerospace Laboratory NLR, Amsterdam, the Netherlands, 2006.

[27] Hoeppner, D.W. and Krupp, W.E. Prediction of component life by application of fatigue crack growth knowledge, *Engineering Fracture Mechanics*, Vol. 6, pp. 47-70, 1974.

[28] Hoeppner, D.W. Personal Communication from the University of Utah, Salt Lake City, Utah, USA, 20 December, 2009.

[29] Paris, P.C. and Erdogan, F. A critical analysis of crack propagation laws, *Journal of Basic Engineering, Transactions of the American Society of Mechanical Engineers*, Series D, Vol. 85, pp. 528-534, 1963.

[30] Various authors in *Corrosion Fatigue: Chemistry, Mechanics and Microstructure*, (editors O.F. Devereux, A.J. McEvily and R.W. Staehle), National Association of Corrosion Engineers, Houston, Texas, USA, 1972.

[31] Various authors in *Corrosion Fatigue of Aircraft Materials*, AGARD Report No. 659, Advisory Group for Aerospace Research and Development, Neuilly-sur-Seine, France, 1977.

[32] Wanhill, R.J.H. Aircraft corrosion and fatigue damage assessment (USAF ASIP publication), NLR Technical Publication TP 95656 U, National Aerospace Laboratory NLR, Amsterdam, the Netherlands, 1995.

[33] Wanhill, R.J.H., Jacobs, F.A. and Schijve, J. Environmental fatigue under gust spectrum loading for sheet and forging aircraft materials, *Fatigue Testing and Design*, (editor R.G. Bathgate), The Society of Environmental Engineers, Vol. 1, pp. 8.1-8.33, Buntingford, UK, 1976.

[34] Schijve, J., Jacobs, F.A. and Tromp, P.J. Environmental effects on crack growth in flight-simulation tests on 2024-T3 and 7075-T6 material, NLR Technical Report TR 76104 U, National Aerospace Laboratory NLR, Amsterdam, the Netherlands, 1976.

[35] Wanhill, R.J.H. Flight simulation environmental fatigue crack propagation in 2024-T3 and 7475-T761 aluminium, *ICAS Proceedings 1980: 12th Congress of the International Council of the Aeronautical Sciences*, (editors J. Singer and R.W. Staufenbiel), American Institute of Aeronautics and Astronautics, Inc., New York, New York, USA, pp. 645-651, 1980.

[36] Wanhill, R.J.H., Jacobs, F.A. and Schra, L. The effect of environment on fatigue crack propagation under gust spectrum loading in aluminium alloy sheet, and the significance for realistic testing, *The Influence of Environment on Fatigue*, The Institution of Mechanical Engineers, London, UK, pp. 101-109, 1977.

[37] Murakami, Y. and Endo, M. Effects of hardness and crack geometries on ΔK_{th} of small cracks emanating from small defects, *The Behaviour of Short Fatigue Cracks, EGF1*, (editors K.J. Miller and E.R. de los Rios), Mechanical Engineering Publications Ltd, London, UK, pp. 275-293, 1986.

[38] Barter, S., Molent, L. and Robertson, L. Using in-service F/A-18 A / B aircraft fatigue cracking as disclosed by teardown to refine fleet life limits. *Proceedings of the 2009 USAF Structural Integrity Program (ASIP) Conference*, Jacksonville, Florida, USA, 30 November - 2 December 2009.

Appendix A: Exceptions to Exponential FCG

A.1. Introduction

In section 2 of this report it was stated that approximately exponential FCG of lead cracks is subject to several conditions. These conditions are:

(a) Little error is made when assessing the EPS of the fatigue-initiating discontinuity. An underestimate will cause a small temporary departure from an exponential trend near the commencement of FCG.

(b) The crack does not grow into an area with a significant thickness change, particularly if the crack length/depth is small compared to the specimen or component thicknesses or widths.

(c) The crack is not unloaded, either (i) by the cracked area losing stiffness and shedding load to other areas of the specimen, component or structure; or because it grows (ii) under bending loads towards a neutral axis or (iii) away from a stress concentration such as a pin-loaded hole in a milti-pin joint such as a wing skin to spar attachment.

(d) The crack does not encounter a significantly changing stress field by growing into or from an area containing residual stresses.

(e) FCG is not retarded by infrequent very high loads (usually in excess of 1.2 X the peak load in the load history).

(f) The small fraction of FCG life influenced by quasi-static fracture close to final failure is ignored.

These conditions are discussed with examples in subsections A.2 to A.7.

A.2. Discontinuity equivalent pre-crack size (EPS) and early FCG

Fatigue-initiating discontinuities typical of those found in aircraft components are usually microscopic and sometimes irregular in shape[8]. This can make it difficult to judge how crack-like[9] they are and to determine an equivalent pre-crack size (EPS), even though there is a well-established empirical expression for converting discontinuity surface areas into EPS values [A.1].

One way to estimate the crack-like effectiveness of a discontinuity is to obtain QF data over a wide range of lead crack sizes and back-extrapolate from the later exponential FCG to zero lifetime to determine the EPS. Although this approach would appear to be completely subjective, there is evidence to support it, certainly for aluminium alloys. This is illustrated by the example in Figure A.1.

Figure A.1a shows plots of log crack depth *versus* linear life for several cracks without accounting for the depths of the initial discontinuities. The starting points for the plots were the beginning of FCG, and the QF measurements showed that FCG began after part of the first flight block. The early FCG data clearly do not follow the later exponential trend. However, when the best estimates of the discontinuity depths are added to the plots *at zero lifetime* and for all subsequent crack depths, Figure A.1b, an approximately exponential FCG trend is found over the whole range of crack sizes.

---

[8] This excludes the rare and exceptional flaws that may be classed as “rogue flaws”.

[9] The propensity of a discontinuity to nucleate or become a fatigue crack.

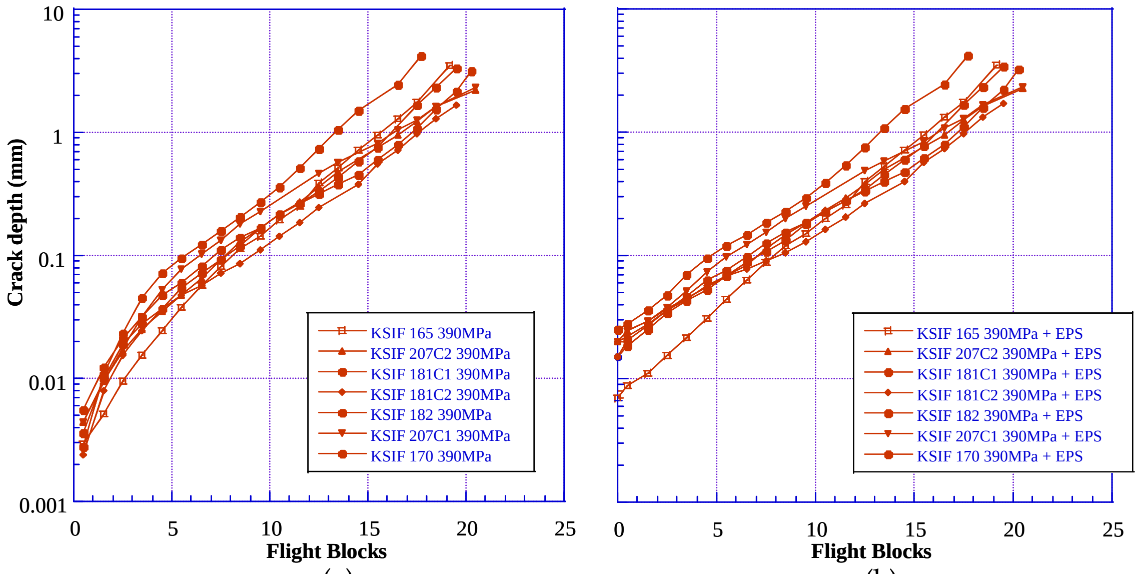

(a) (b)

Figure A.1: FCG data for AA7050-T7451 aluminium alloy coupons tested under combat aircraft flight-by-flight block loading: (a) without and (b) with corrections to the effective crack depths by adding the initial discontinuity depths at zero lifetime and for all subsequent crack depths [A.2]

A.3. Component thickness and geometry changes

Changes in component thickness and geometry can cause changes in FCG rates. A change from thick to thin sections can increase the FCG rates, while a change from thin to thick sections can decrease the FCG rates.

Such changes often occur late in life, when the cracks are growing rapidly. If so, a departure from approximately exponential FCG is unimportant. However, if the FCG rates are affected earlier, then the general intent would be to use the faster FCG for lifing purposes, to ensure conservative estimates. This is not mandatory: the decision about which FCG data to use would likely be made on a case-by-case basis, bearing in mind that a certain level of conservatism has to be achieved.

Figure A.2 shows an example of a crack growing through a significantly changing geometry, known as the FT46 Y557 kick-point, a location on the upper longeron of an aft fuselage full-scale test article [A.3]. QF measurements resulted in the FCG curve shown in Figure A.3. This plot is exponential until the crack enters the 'Y' junction, whereupon the FCG rate decreased for about 8000 simulated flight hours (SFH). Since exponential FCG pertained over most of the crack growth life, this behaviour was used to provide a conservative estimate of the FCG life for the kick-point location.

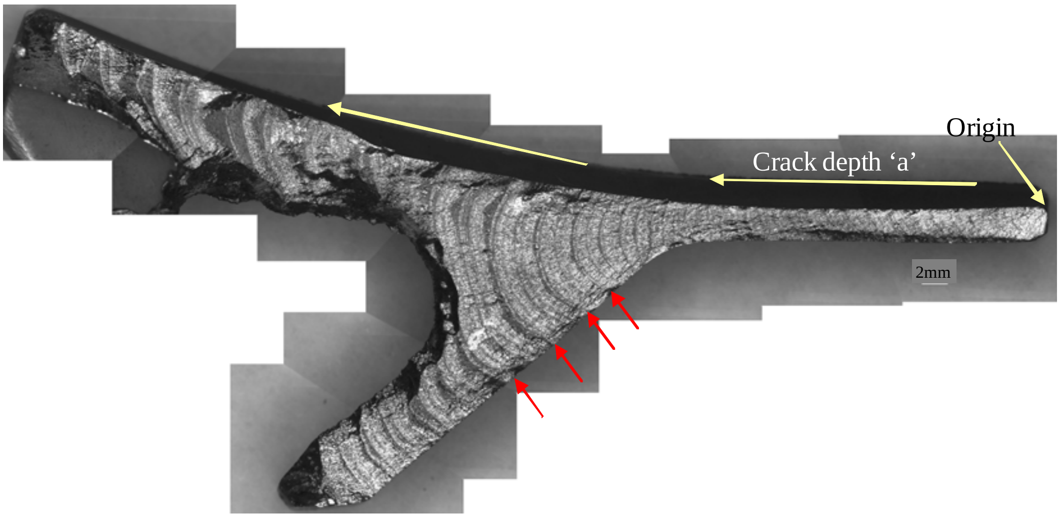

Figure A.2: Optical fractograph of a fatigue crack growing through a major change in geometry, known as the FT46 (AA7050-T7451) Y557 kick-point, under combat aircraft (F/A-18) flight-by-flight block loading [A.3,A.4]. The pattern of the block repeats (some marked by red arrows) was used to generate the FCG curve in Figure A.3. The large arrows indicate the direction of crack measurement.

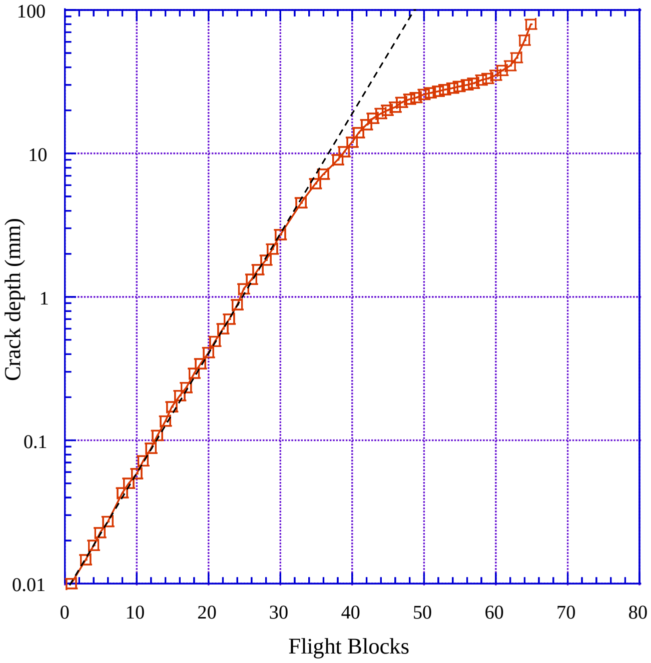

Figure A.3: FCG curve derived for the FT46 Y557 kick-point [A.4]. The commencement of decreasing FCG rates corresponds to the crack entering the ‘Y’ junction, see Figure A.2. The dashed line represents exponential FCG and would give a conservative estimate of the FCG life.

A.4. Load shedding

A.4.1 Load shedding to adjacent areas and structures

A growing fatigue crack may cause the cracked area to lose stiffness and shed loads to other areas of a specimen, component or structure. This may or may not result in (secondary) cracking in these areas, but the stiffness loss will influence the primary crack and cause a deviation from exponential FCG. Two examples will be given here.

Figure A.4 shows QF FCG data for one of the lugs of a wing leading edge lift device from an F/A-18 full-scale wing test [A.5]. The FCG behaviour was approximately exponential for about 32 blocks of simulated flights. The cracked lug then began to shed load, most probably to adjacent lugs, resulting in a decrease in FCG rates. Exponential FCG could still be used to provide a conservative estimate of the FCG life, as is indicated by the dashed line. However, in this case the estimate would be over-conservative, since load shedding prevented the lug from failing during the test.

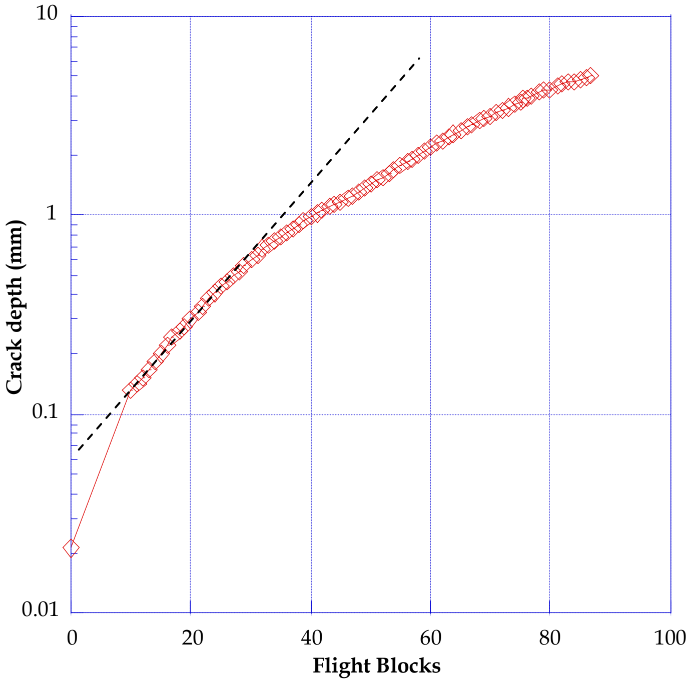

Figure A.4: FCG for an attachment lug of a wing leading edge device from a full-scale F/A-18 wing test [A.5]. Load shedding caused decreased FCG rates after about 32 blocks of simulated flights. The dashed line represents exponential FCG and would give a conservative estimate of the FCG life.

Figure A.5 shows a more complicated example of load shedding. This is from a full-scale fatigue test for the General Dynamics F-111A aircraft, specifically the wing splice area. The splice consisted of a D6ac steel plate fastened to a 2024-T851 aluminium alloy plate.

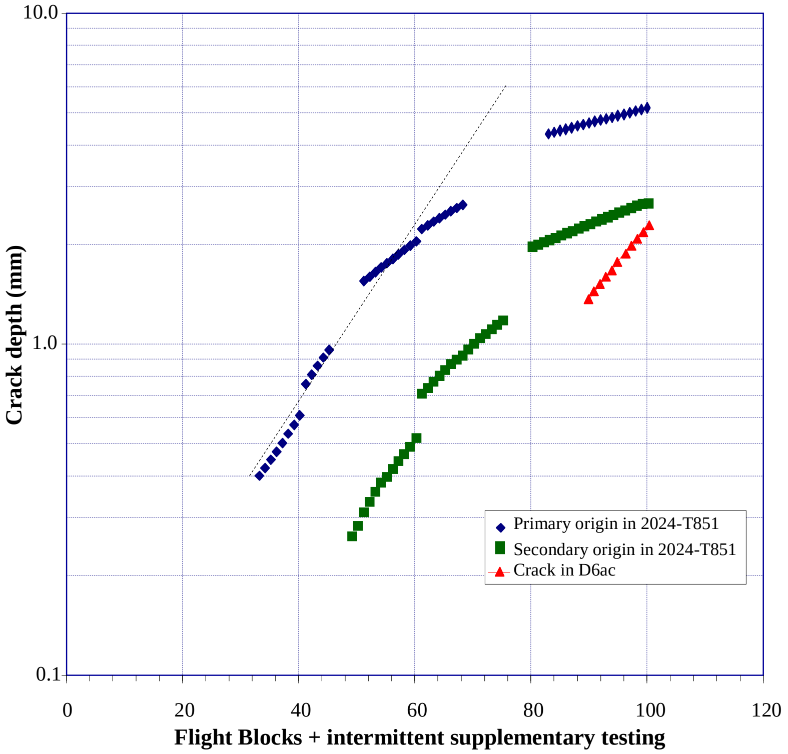

Figure A.5: FCG from fastener hole 182 in the wing pivot splice produced during an F-111A full-scale fatigue test: adapted from [A.1.6]. Step changes in the plots are due to intermittent short-term supplementary testing. The dashed line represents exponential FCG for the crack growing from the primary origin in the AA2024-T851 wing skin would give a conservative estimate of the FCG life.

The FCG behaviour shown in Figure A.5 is due to a combination of load shedding and sequential FCG. Despite this, the earlier exponential FCG for each component of the splice could be used to provide conservative estimates of the FCG lives. For example, the dashed line in Figure A.5 indicates how to obtain a conservative estimate of the FCG life for the primary aluminium alloy plate. However, as in the previous case of a wing leading edge attachment lug, the continuous load shedding would mean an over-conservative estimate of the FCG life.

A.4.2 Load shedding owing to local bending or pin loads

A fatigue crack growing in a local bending field towards the neutral axis will experience load shedding and consequent decreasing FCG rates. This is also the case when a crack grows away from a stress concentration, notably from a pin-loaded hole in a multi-pin attachment. An example of the latter, albeit with an additional load shedding effect, is given here.

Figure A.6 shows QF FCG data for a crack growing from one of the bolt holes in an aluminium alloy wing spar during an F/A-18 full-scale wing test [A.7]. The spar was bolted to a much stiffer carbon fibre composite wing skin. This meant that not only was the crack growing away from a stress concentration (the bolt hole), but there was also load shedding from the spar to the wing skin. Despite these effects the FCG data show approximately exponential behaviour for most of the test history, enabling a reasonably conservative estimate of the FCG life, as is indicated by the dashed line.

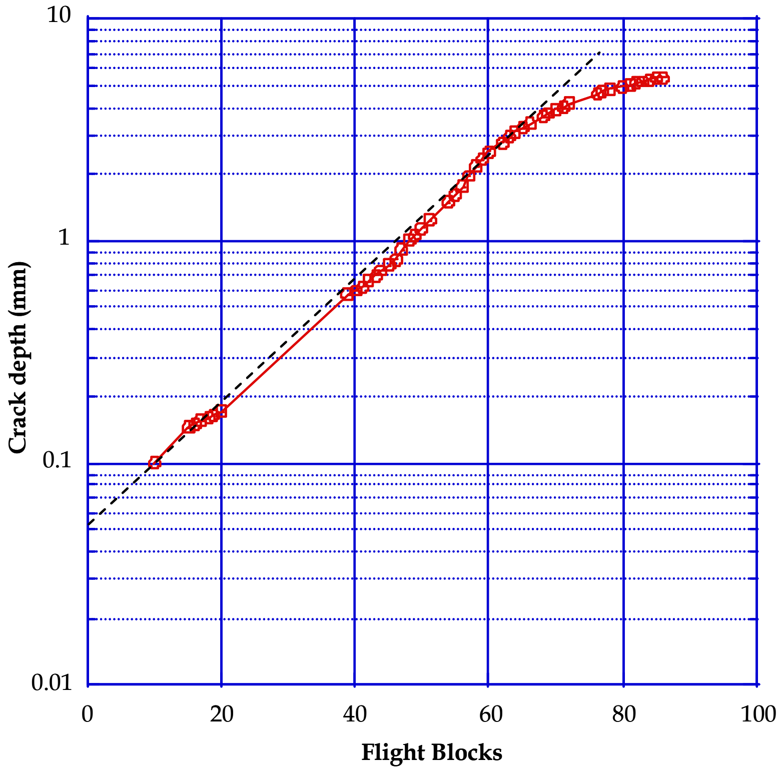

Figure A.6: FCG from a bolt hole in an aluminium alloy outer wing spar during a full-scale F/A-18 wing fatigue test [A.7]. Load shedding caused decreased FCG rates after about 60 blocks of simulated flights. The dashed line represents exponential FCG and would give a reasonably conservative estimate of the FCG life.

A.5. Residual stresses

Residual stresses are generally ill-defined or unknown. However, quantifiable residual stresses are sometimes introduced into components to improve the fatigue life. Typical applications are the use of interference fit fasteners and shot peening.

Figure A.7 is an example of FCG influenced by shot (glass bead) peening which introduced compressive residual stresses to a depth of about 0.25 mm. Each FCG curve consists of two segments of approximately exponential behaviour. The difference between the slopes of the segments, i.e. the exponent values, is most pronounced at the lowest fatigue stress levels.

This example shows that approximately exponential FCG behaviour is possible within a residual stress field. In such cases a piecewise exponential approach can be used to estimate the FCG life [A.9].

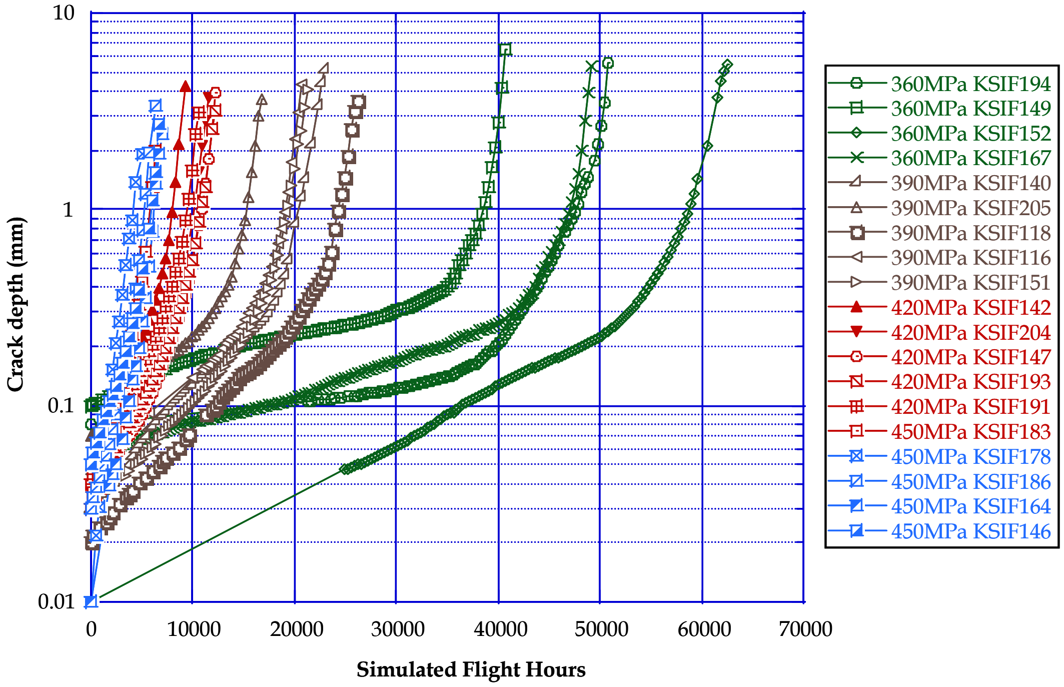

Figure A.7: FCG data for shot peened AA7050-T7451coupons tested under combat aircraft flight-by-flight block loading at several stress levels [A.8].

A.6. FCG retardation due to peak loads

FCG retardation after the occurrence of a peak load is well-known, and has been extensively studied, e.g. [A.10]. This phenomenon is especially pronounced for FCG in thin sheets of naturally aged (T3X and T4) 2XXX aluminium alloys subjected to gust spectrum load histories at stress levels typical for transport aircraft structures. On the other hand, retardation is much less evident in thicker sections of artificially aged (T6X and T7X) 7XXX aluminium alloys subjected to manoeuvre spectrum loading at stress levels typical for combat aircraft structures.

There are two main reasons for these material and load history influences on FCG retardation. Firstly, higher strengths and thicker sections reduce the extent of crack tip plasticity due to peak loads and hence the size of the zone affected by retardation. Secondly, manoeuvre load histories contain many more high loads of similar magnitude. The overall effect is for crack growth to be a quasi-stationary process, resulting in regular FCG curves. This is the case in the context of the present report, as may be seen from the regular FCG curves in Figures 1 and 3 and from Figures A.1 − A.7.

That FCG retardation *does* occur during quasi-stationary FCG is illustrated by the following example. Figure A.8 shows a FCG curve for a 7050-T7451 aluminium alloy specimen subjected to a simple load sequence consisting of blocks of 200 cycles of CA loading separated by single peak load cycles. The overall FCG behaviour was exponential until the crack became relatively large with respect to the specimen dimensions. Even then, the crack growth curve remained highly regular.

However, QF examination, e.g. Figure A.9, showed that the peak loads resulted firstly in an increase in FCG rate (wider fatigue striations), followed by a decline in FCG rate to below the stable CA level, and then a gradual increase in FCG rate to this level. Nevertheless, these pronounced local variations in FCG rate did not affect the overall behaviour.

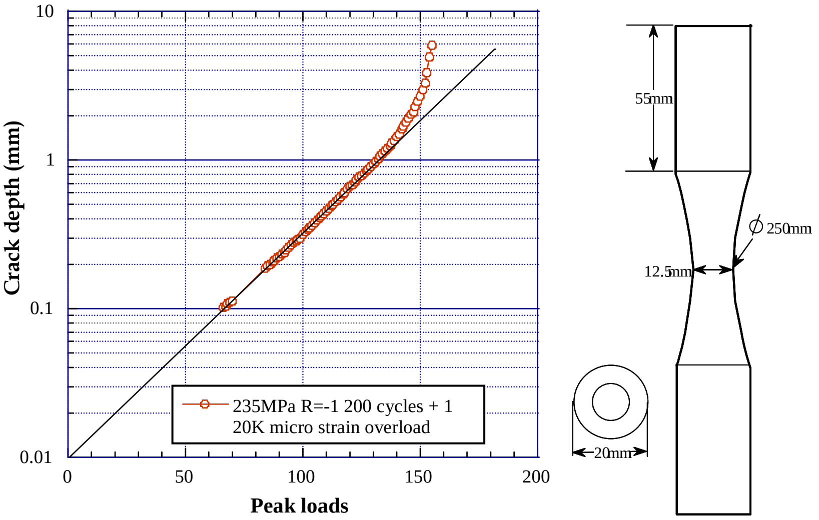

Figure A.8: FCG data for an AA7050-T7451 aluminium alloy cylindrical specimen subjected to a load sequence of blocks of 200 cycles of CA loading separated by single peak load cycle.

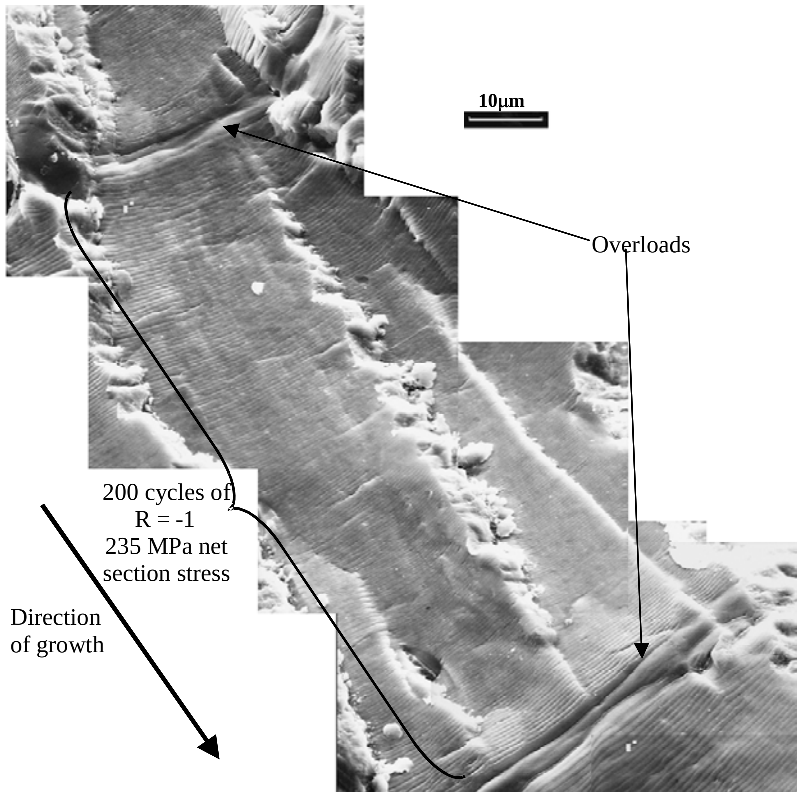
10μm
Overloads
200 cycles of
R = -1
235 MPa net
section stress
Direction
of growth

Figure A.9: QF view of part of the fatigue fracture surface of the specimen illustrated in Figure A.8.

The question of whether exponential FCG could apply to transport aircraft structures, which are less highly loaded and experience mainly gust load histories, has yet to be investigated in detail. However there is data that suggest this is generally not so [A.10,A.11]. More direct evidence is provided by Figure A.10. This shows FCG curves for 2024-T3 aluminium alloy panels subjected to gust spectrum flight-by-flight block loading at three stress levels. Only at the highest stress level does the FCG behaviour appear to be approximately exponential, but this stress level is much too high for application in a transport aircraft structure. Nevertheless, exponential approximations such as those fitted to the lower stress level data may be useful to provide first-order life assessments for these stress levels.

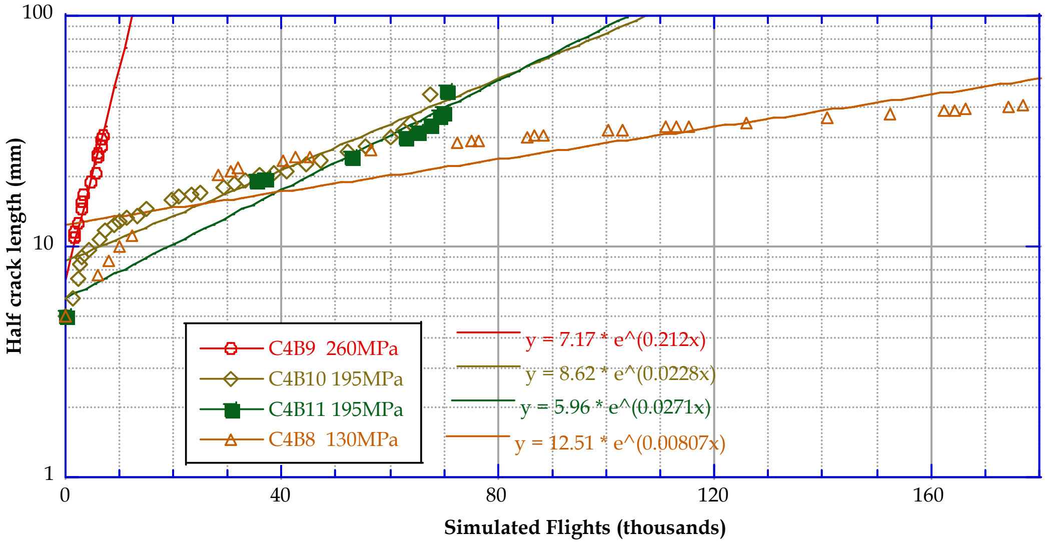

Figure A.10:FCG data for AA2024-T3 panels subjected to the standard gust spectrum loading, TWIST [A.12]. The data are replotted from [A.13].

A.7. Quasi-static fracture close to final failure

While exponential FCG is a reasonable approximation for lead cracks over most of the crack growth life, there is an acceleration causing an upturn of the FCG curves towards the end of life. This acceleration is partly due to the onset of quasi-static fracture by microvoid coalescence, and is also a consequence of geometrical influences on the crack driving force, i.e. finite geometry effects on the crack tip stress intensity factors. These two factors are related, since higher crack tip stress intensity factors promote quasi-static fracture.

Figure A.11 shows FCG curves for aluminium alloy panels subjected to manoeuvre spectrum flight-by-flight block loading at two stress levels. In all cases the FCG is approximately exponential until relatively late in life. Furthermore, if one were to apply the 1.2DLL failure criterion, then the upturns in the FCG curves would be clipped, since the coupons would most probably not have survived this load.

In other words, whether or not quasi-static fracture and FCG curve upturns occur, it is reasonable for the lead crack fatigue lifing framework to generally ignore these phenomena and assume approximately exponential FCG for the entire crack growth life.

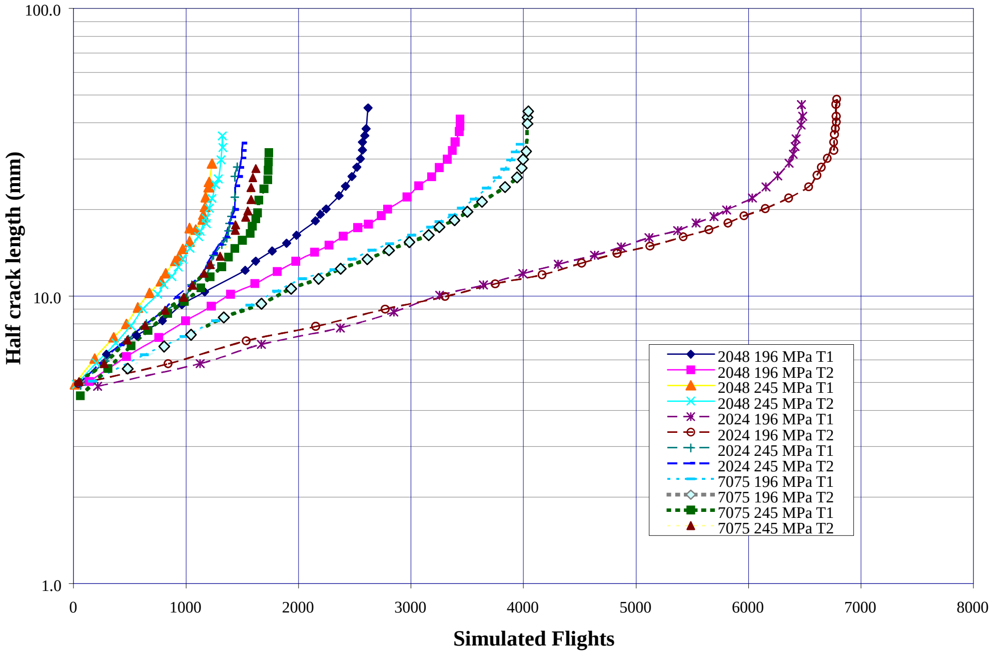

Figure A.11:FCG data for AA2048-T851, AA2024-T3 and AA7075-T6 aluminium alloy panels subjected to the standard manoeuvre spectrum loading, FALSTAFF [A.14]. The data are replotted from [A.10].

A.8. References

[A.1] Murakami, Y. and Endo, M. Effects of hardness and crack geometries on ΔK_{th} of small cracks emanating from small defects, *The Behaviour of Short Fatigue Cracks, EGF1*, (editors K.J. Miller and E.R. de los Rios), Mechanical Engineering Publications Ltd, London, UK, pp. 275-293, 1986.

[A.2] Barter, S.A. The fatigue of a high strength aluminium alloy in air – quantitative fractographic methods and life prediction, *PhD Dissertation*, Monash University, Melbourne, Australia, 2008.

[A.3] Simpson, D.L., Landry, N., Roussel, J., Molent, L., Graham, A.D. and Schmidt. N. The Canadian and Australian F/A-18 international follow-on structural test project, *ICAS Proceedings 2002: 23rd Congress of the International Council of the Aeronautical Sciences*, (editor I. Grant) Toronto, Canada, 2002.

[A.4] Barter, S.A. Right hand side centre section of the upper longeron at Y557 kick-point, DSTO Fractographic Analysis Report FFT46-0042, Defence Science and Technology Organisation, Melbourne, Australia, 2003.

[A.5] Barter, S.A. Outer wing forward spar, DSTO Fractographic Analysis Report FT93L0017, Defence Science and Technology Organisation, Melbourne, Australia, 2004.

[A.6] Wolanski, Z.R. F-111A Airframe fatigue test program left hand wing component test, metallurgical analysis of the lower skin failure, Report FZS-12-327, General Dynamics Convair Aerospace Division (now Lockheed Martin), Fort Worth, Texas, USA, 1972.

[A.7] Barter, S.A. Outer wing no. 3 spar, DSTO Fractographic Analysis Report FT93L0017, Defence Science and Technology Organisation, Melbourne, Australia, 2004.

[A.8] Barter, S.A. Fatigue crack growth in 7050T7451 aluminium alloy thick section plate with a glass bead peened surface simulating some regions of the F/A-18 structure, DSTO Technical Report DSTO-TR-1477, Defence Science and Technology Organisation, Melbourne, Australia, 2003.

[A.9] Molent, L., Barter, S. and Main, B. Life assessment and repair of fatigue damaged high strength aluminium alloy structure using a peening rework method, *Engineering Failure Analysis*, Vol. 15, pp. 62-82, 2008.

[A.10] Wanhill, R.J.H. Damage tolerance engineering property evaluations of aerospace aluminium alloys with emphasis on fatigue crack growth, NLR Technical Publication TP 94177, National Aerospace Laboratory NLR, Amsterdam, the Netherlands, 1995.

[A.11] Wanhill, R.J.H., Hattenberg, T. and van der Hoeven, W. A practical investigation of aircraft pressure cabin MSD fatigue and corrosion, NLR Contract Report NLR-CR-2001-256, National Aerospace Laboratory NLR, Amsterdam, the Netherlands, 2001.

[A.12] De Jonge, J.B., Schütz, D., Lowak, H. and Schijve, J. A standardized load sequence for flight simulation tests on transport aircraft wing structures, NLR Technical Report TR 73029 U, National Aerospace Laboratory NLR, Amsterdam, the Netherlands, 1973.

[A.13] Wang, G.S. and Blom, AF. A strip model for fatigue crack growth predictions under general load conditions, *Engineering Fracture Mechanics*, Vol. 40, pp. 507-533, 1991.

[A.14] Anon. Description of a Fighter Aircraft Loading STAndard For Fatigue evaluation, Combined Report of the F+W, LBF, NLR and IABG, 1976.

Appendix B: Fatigue-initiating Discontinuities

B.1. Introduction

As stated in section 3 of this report, under more or less ideal conditions a significant period of fatigue-induced microstructural damage can precede fatigue crack initiation. However, production aircraft components and structures have many sources of surface or near-surface discontinuities capable of causing fatigue cracking very quickly in highly stressed locations and areas.

The discontinuities include various forms of machining damage (scratches, grooves, burrs, small tears and nicks); etch pits from surface treatments (pickling, anodising); porosity, especially in thick aluminium alloy plate and castings; and in the case of aluminium alloys and steels, constituent particles that may themselves be cracked.

Table B.1 lists examples of fatigue-initiating discontinuities to be discussed in subsection B.2. These examples are representative of those capable of starting lead fatigue cracks and have been selected from a variety of aircraft types and for various fatigue conditions. Most are for aluminium alloys owing to their widespread use in metallic airframe structures. This is also the reason why fatigue crack initiation in aluminium alloys is reviewed in subsection B.3.

Table B.1: Overview of examples of fatigue-initiating discontinuities

Discontinuity sources	Specifics	Aircraft type	Fatigue conditions
poorly finished holes	poor drilling	Aermacchi MB326	FSFT
		Airbus A380 MLB**	FSFT
	scoring from fastener	Aermacchi MB326	service
	poor de-burring	Aermacchi MB326	service
	machining tears/nicks	Aermacchi MB326	service and FSFT
		Dassault Mirage III	service
		Boeing F/A-18A/B	coupon test
		Lockheed P3C	FSFT
surface treatments	etch pits	Boeing F/A-18A/B	coupon tests
	etch pits + machining	Boeing F/A-18A/B	service
	intergranular "penetration"	Boeing B747	service
	chemical milling + peening	General Dynamics F-111	service and FSFT
	pickling	Lockheed P3C	FSFT
	peening laps and cuts	Boeing F/A-18A/B	coupon tests
porosity	thick plate porosity	Boeing F/A-18A/B	FSFT
constituent particles	cracked particles	–	coupon test
	varying shapes	Boeing F/A-18A/B	coupon tests
	particles + poor machining	Dassault Mirage III	FSFT

* FSFT = Full-Scale Fatigue Test ** MLB = MegaLiner Barrel

Most of the discontinuities listed in table B.1 are typical of a normal production environment. The occurrence of poorly finished holes and peening defects can be avoided to some extent by closer control. However, production improvements are limited owing to the generally small size of the discontinuities, making them hard to detect by pre-service NDI. Other types of discontinuity are simply unavoidable, e.g. etch pits from chemical treatments, porosity in castings (which have only limited use in primary airframe structures), and the constituent particles in aluminium alloys and steels.

B.2. Examples of discontinuities

B.2.1 Poorly finished holes

Table B.2 lists the examples: examples 1, 3−5 are from Aermacchi MB326 trainers, now retired from RAAF service; example 2 is from a full-scale fatigue test of the Airbus MegaLiner Barrel (MLB); example 6 is from a Dassault Mirage III, also withdrawn from service; example 7 is from coupon tests used to support the Boeing F/A-18A/B lifing programme; examples 8 and 9 are from a full-scale test of the Lockheed P3C empennage.

Table B.2: Examples of fatigue-initiating discontinuities: poorly finished holes

Discontinuity description	Component	Aircraft type	Fatigue	Example	Ref.
drilling: gross damage, tearing, scoring fastener insertion: scoring bad de-burring machining tears	AA7075-T6 main spar	Aermacchi MB326	FSFT	1	[B.1]
	GLARE* door beam	Airbus MLB	FSFT	2	[B.2]
	AA7075-T6 main spar	Aermacchi MB326	service	3	[B.1]
	AA7075-T6 main spar	Aermacchi MB326	service	4	[B.1]
	AISI 4340 carry-through beam	Aermacchi MB326	service	5	[B.3]
	AU4SG** spar	Dassault Mirage III	service	6	[B.4]
	AA7050-T7451 coupon	Boeing F/A-18A/B	test	7	[B.5]
	AA7075-T6 empennage	Lockheed P3C	FSFT	8	[B.6]

*GLARE = GLAss REinforced aluminium laminates **AU4SG ≡ AA2014-T6

Example 1: Figure B.1 shows the fatigue cracking, which started on both sides of the fastener hole at the beginning of the FSFT and ultimately failed the wing main spar. On the right-hand side of the hole (as shown in the figure) three cracks (arrowed) grew from gross drill-damage. These cracks interacted and coalesced, and hence grew faster than a single crack growing from a drill-induced tear on the left-hand side. The arrow on this side indicates the extent of this crack when the right side failed.

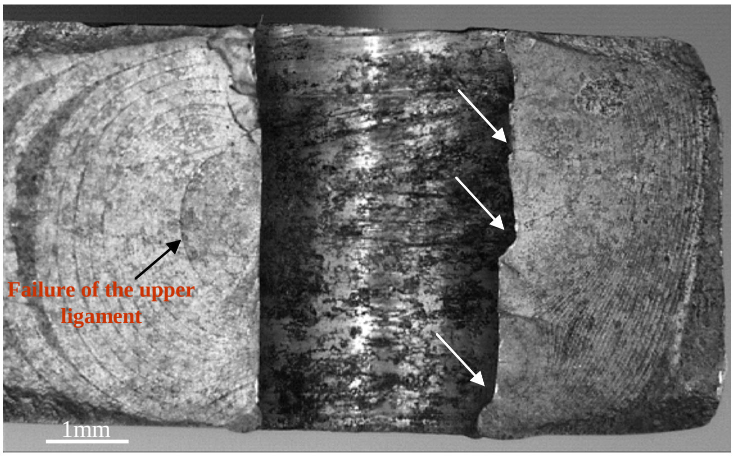

Figure B.1: Example of a poorly drilled hole in a main wing spar made from an AA7075-T6 aluminium alloy extrusion. The cracking on the right side of the hole has initiated from gross drill damage, while the crack on the left side of the hole initiated from a drill-induced surface tear during machining.

Example 2: Figure B.2 shows FSFT fatigue cracks in the bore of a GLARE fastener hole in the MLB passenger door beam. Most cracks grew from the 2024-T3 aluminium alloy sheet corners [B.2], but in this example a crack also started from scoring owing to poor drilling. This result and other evidence of poor drilling led to a production improvement programme for GLARE components in the Airbus A380.

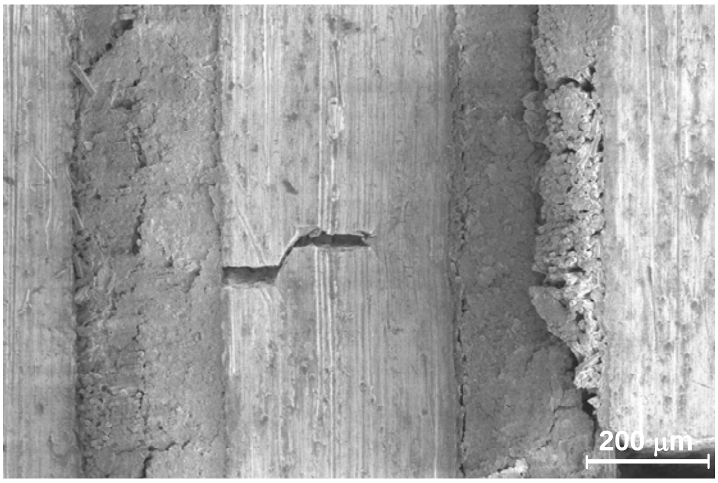

Figure B.2: Example of fatigue cracking initiating from scoring in the bore of a fastener hole in the MLB GLARE door beam [B.2]. The cracking is in one of the AA2024-T3 sheets of the GLARE laminate.

Example 3: Figure B.3 shows service fatigue cracks starting from scoring along the bore of a fastener hole in a wing main spar. The scoring was due to insertion of a blind fastener. The cracks grew more or less evenly on both sides of the hole, and would probably have failed the spar if it had remained in service. Discovery of these cracks led to an extensive teardown programme, and many similarly damaged holes were found [B.1].

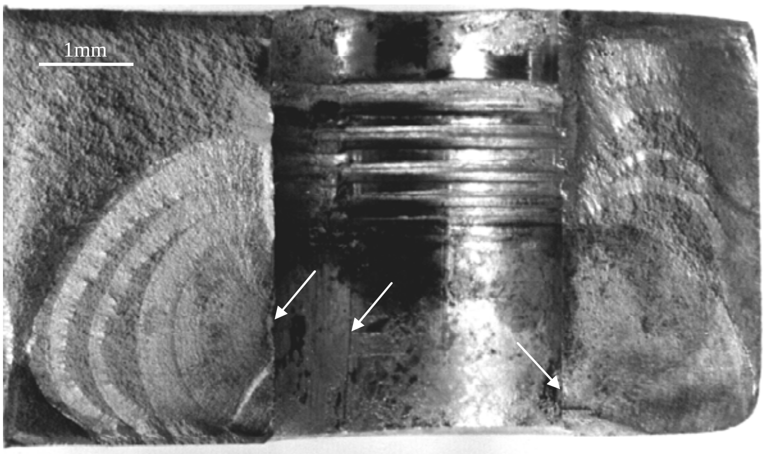

Figure B.3: Example of a hole that was damaged by fastener insertion in a main wing spar made from an AA7075-T6 extrusion. Service fatigue cracks have initiated from surface scores produced during insertion of a blind fastener. The middle arrow (bore of the hole) indicates one of the scores.

Example 4: Figure B.4 shows service fatigue cracks growing from a fastener hole in a wing main spar withdrawn from service. The hole had been badly de-burred, resulting in a split burr that started the upper crack and several nicks (arrowed), one of which started the lower crack. These cracks were found during the teardown programme mentioned in example 3 [B.1].

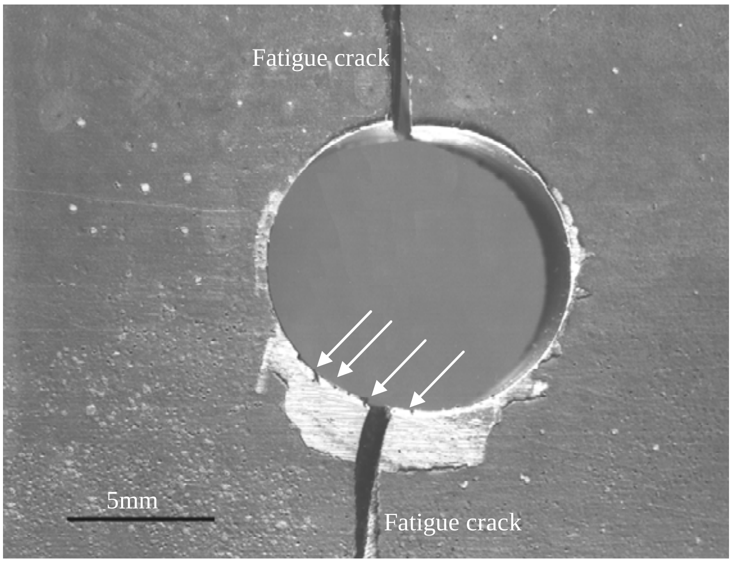

Figure B.4: Example of a hole that was poorly finished in a main wing spar made from an AA7075-T6 extrusion. The upper fatigue crack initiated from a split in a burr at the edge of the hole. The lower fatigue crack initiated from a nick on the edge of the hole: other nicks are indicated by the small arrows.

Example 5: Figure B.5 shows magnetic rubber casts of service fatigue cracks growing from machining tears in two fastener holes. These were from steel centre-section lower beams of wing carry-through frames, and were detected during a safety-by-inspection programme. This programme enabled the aircraft to remain in service until the cracks reached unacceptable sizes, at which time either (a) the holes were oversized to remove the cracking, or (b) the centre-section beams were replaced, or (c) the aircraft were retired, depending on the overall life in service [B.3].

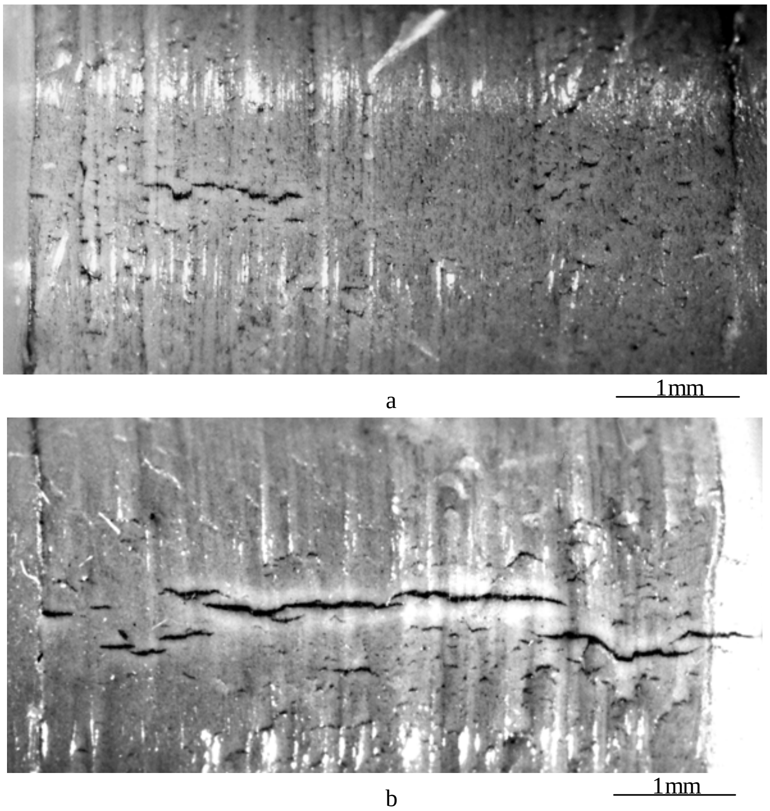

Figure B.5: Two examples of fastener holes in an AISI 4340 steel wing carry-through beam. The views are of magnetic rubber casts of the holes and show indications of machining tears and associated fatigue cracks.

Example 6: Figure B.6 shows service fatigue cracks growing from machining tears in a severely damaged fastener hole in a wing spar withdrawn from service [B.4]. The fastener hole damage included tears, laps and deep grooves, and the fatigue-starting tears were usually associated with laps, as in this example.

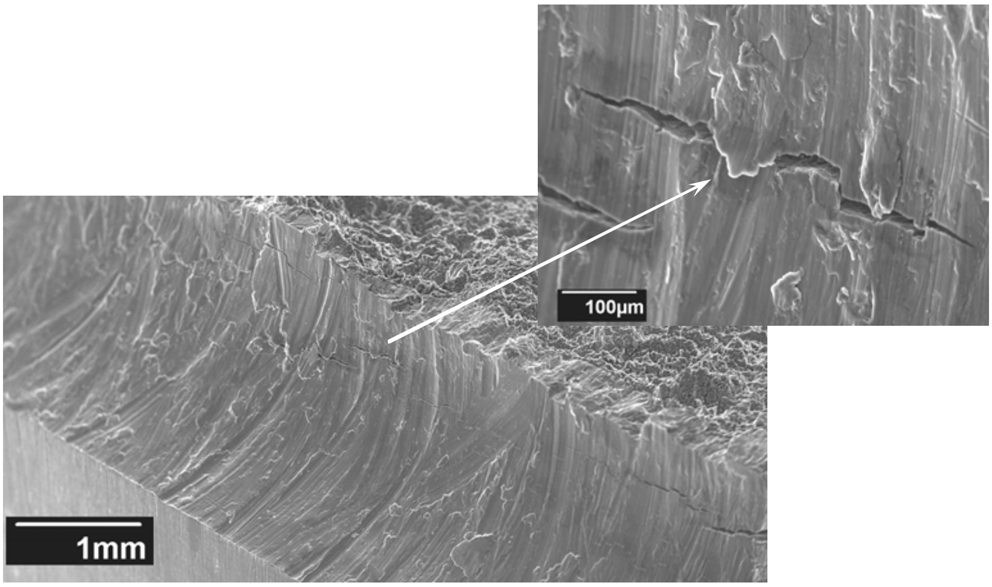

Figure B.6: Example of service fatigue cracking in a poorly drilled hole in an AU4SG aluminium alloy wing spar.

Example 7: Figure B.7 shows a coupon test fatigue crack growing from one of several machining tears (arrowed) in a fastener hole. The tears were associated with one of a series of long, shallow grooves inside the hole [B.5]. This example is also shown as Figure 2A in subsection 3.1 of this report.

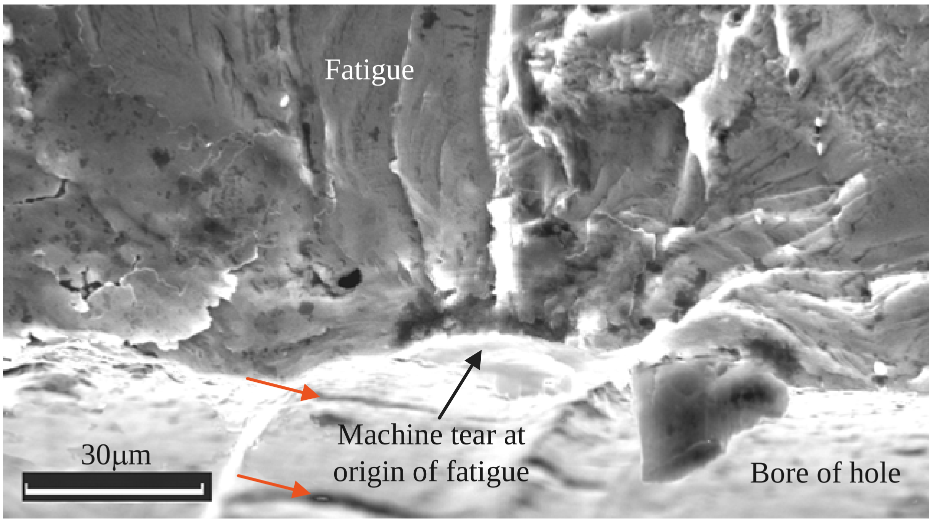

Figure B.7: Fatigue cracking initiating from a shallow long surface groove combined with a machining tear in an AA7050-T7451 coupon.

Example 8: Figure B.8 shows an FSFT fatigue crack that started from one of several small tears at the lip of a fastener hole. The fastener hole was in an empennage aluminium alloy extrusion. Similar tears and associated fatigue cracks were found at other fastener holes in the empennage [B.6].

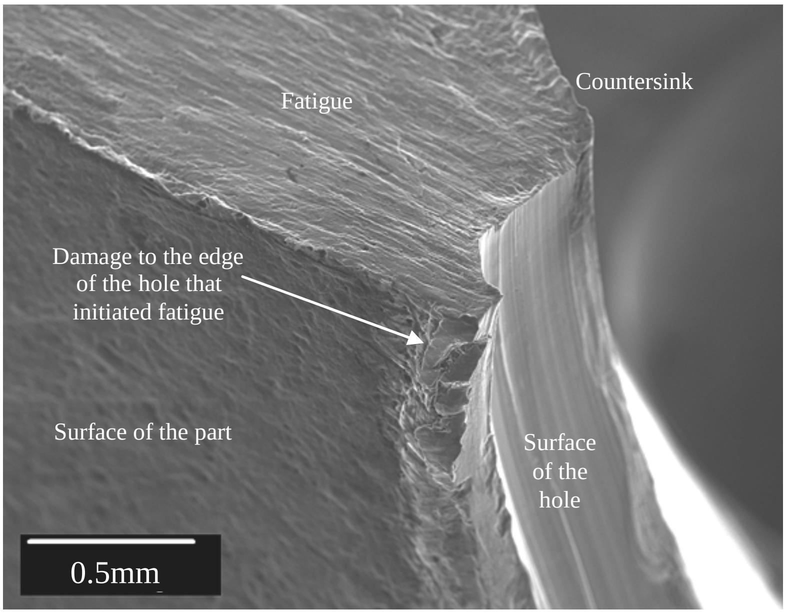

Figure B.8: Fatigue cracking initiating from damage to a lip that surrounded a countersunk hole in an empennage extrusion made from AA7075-T6.

B.2.2 Surface treatments

This subsection contains examples of chemical treatments and also one on shot peening, see Table B.3. There is a wide variety of chemical treatments, which include pickling, anodising and chemical milling. All these treatments can have detrimental influences on fatigue initiation, but - within limits - this must be accepted. However, shot peening can be used both for surface cleaning and to improve the fatigue life, see subsection A.5.

Table B.3: Table B.3 Examples of fatigue-initiating discontinuities: surface treatments

Discontinuity description	Component	Aircraft type	Fatigue	Example	Ref.
etch pits (pickling)	AA7050-T7451 coupon	Boeing F/A-18A/B	test	9	[B.7]
etch pits + machining	AA7050-T7451 bulkhead	Boeing F/A-18A/B	FSFT	10	[B.8]
intergranular attack	AISI 4340M trunnion	Boeing B747	service	11	[B.9]
chemical milling	AA2024-T851 wing skin	G. D.* F-111	FSFT	12	[B.10]
de-oxidising (pickling)	AA7075-T6 empennage	Lockheed P3C	FSFT	13	[B.6]
peening	AA7050-T7451 coupon	Boeing F/A-18A/B	test	14	[B.11]

*G.D. = General Dynamics (now Lockheed Martin)

Pickling, anodising and chemical milling are common treatments for aluminium alloys, and they can all cause etch pits. The composition of the alloy, manufactured condition (e.g. plate, forgings and extrusions) and heat-treatment can all influence the size and nature of the pits, which are usually at grain boundaries and surface-breaking constituent particles. These may be removed during the treatments, resulting in angular pits. The shapes of the pits, particularly their depth profiles, determine the ease with which fatigue cracks initiate and start to grow.

Besides pitting, grain boundary attack or even cracking can result from chemical treatments, notably in high strength steels. These grain boundary "penetrations" have sharp tips that allow FCG to commence as soon as the components are subjected to service loads. Example 11 is a good illustration of this.

Example 9: Figure B.9 shows coupon test fatigue cracks growing from small angular etch pits [B.7]. The coupons were pickled using a treatment applied to much of the primary structure of the F/A-18A/B aircraft.

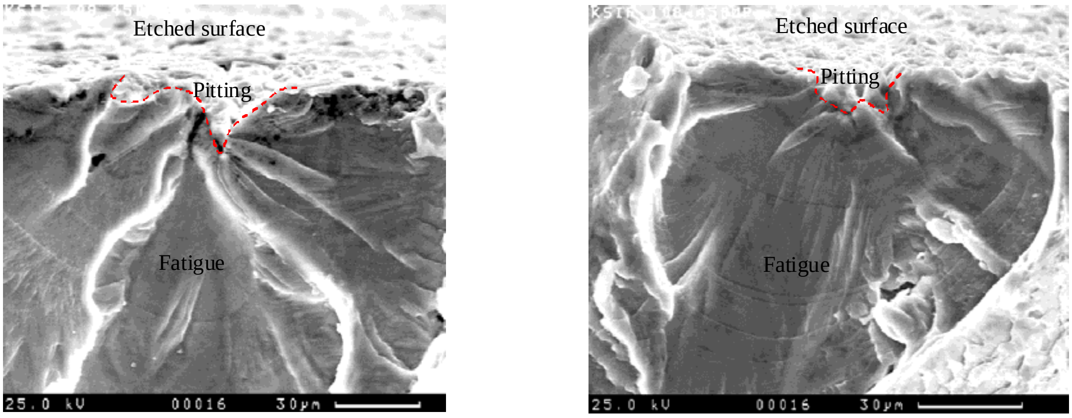
Etched surface
Pitting
Fatigue
25.0 kV
00016
30µm
Etched surface
Pitting
Fatigue
25.0 kV
00016
30µm

Figure B.9: Two fatigue cracks that initiated from etch pits on coupons made from AA7050-T7451. Red outlines give the approximate interfaces between the flaws and the beginning of fatigue crack growth.

Example 10: Figure B.10 shows FSFT fatigue cracks growing from small etch pits in shallow depressions due to coarse machining marks. The cracks occurred during a test on an F/A-18 wing attachment bulkhead. The coarse machining marks apparently contributed to the fatigue-severity of the etch pits, since the fatigue cracks had shorter lives than similarly-located ones in other bulkheads without the machining marks [B.8].

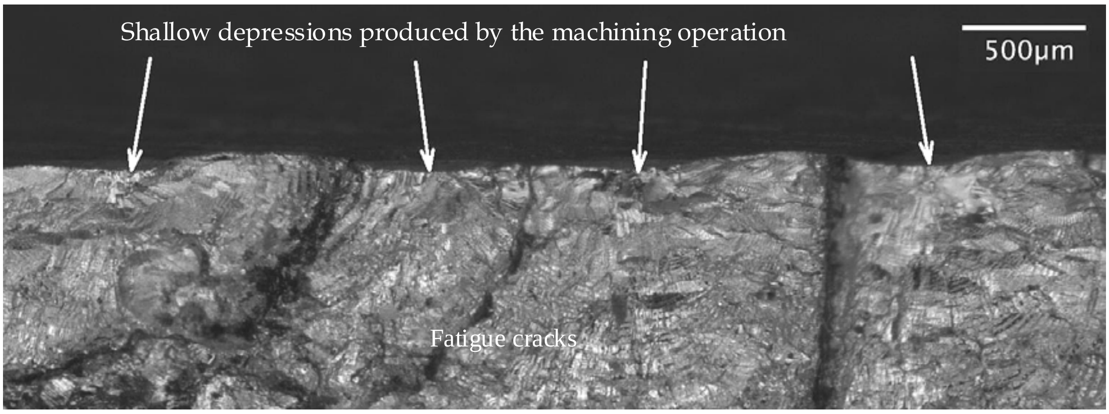
Shallow depressions produced by the machining operation
500µm
Fatigue cracks

Figure B.10: Example of a fatigue test failure in a full-scale fatigue test article. Multiple fatigue cracking started from small etch pits at the base of coarse machining grooves. The material was AA7050-T7451 plate.

Example 11: Figure B.11 shows a small intergranular penetration and subsequent service fatigue cracking in a high strength steel landing gear trunnion from a Boeing B747. The penetration was caused by a black oxide coating process, and its fatigue-severity was augmented by coarse machining and omission of shot peening before the coating was applied [B.9].

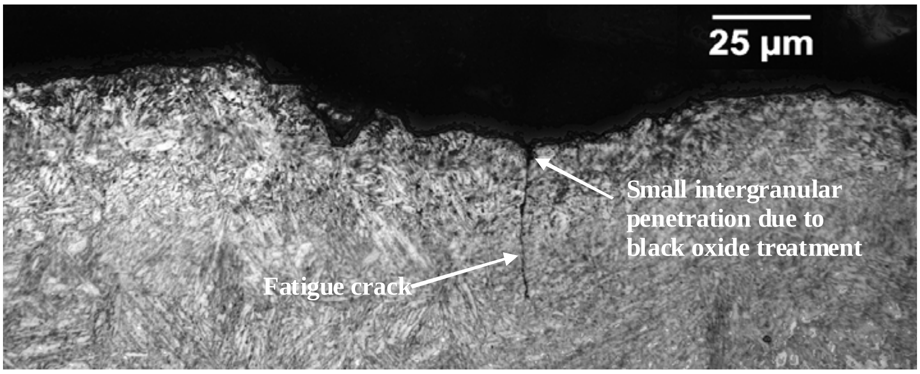
25 µm
Small intergranular penetration due to black oxide treatment
Fatigue crack

Figure B.11: Example of a service fatigue crack starting from a small intergranular surface penetration caused by a black oxide coating process. The penetration was at the base of a coarse machining groove on a landing gear trunnion made from AISI 4340M ultrahigh strength steel. The trunnion surface had not been shot peened (as required) prior to the black oxide treatment.

Example 12: Figure B.12 shows an FSFT fatigue crack growing from small etch pits on the chemically milled and peened surface of a wing lower skin. The peening was most probably inadequate since the etch pits were clearly visible. Also, the location was a shallow radius where peak stresses were very high. The crack shown in Figure B.12 failed the wing during the test, i.e. it was the lead crack. Similar cracks were found in the fleet [B.10].

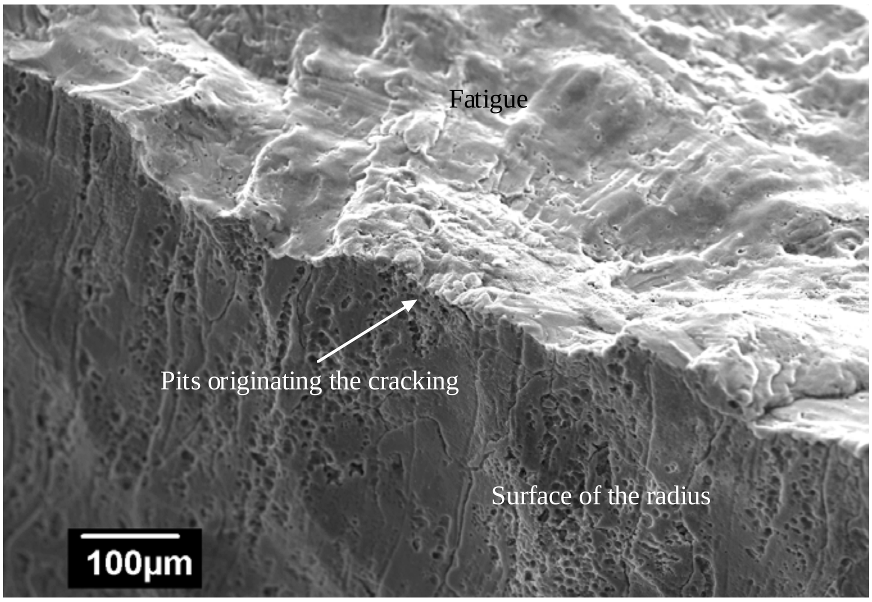

Figure B.12: Example of fatigue cracking from small etch pits during the FSFT of an AA2024-T851 wing lower skin. Cracking from the etch pits may have been facilitated by a shallow radius in the skin.

Example 13: Figure B.13 shows an FSFT fatigue crack growing from etch pits due to a de-oxidising treatment applied to many P3C components before anodising. This example is from an aluminium alloy extrusion in the empennage [B.6].

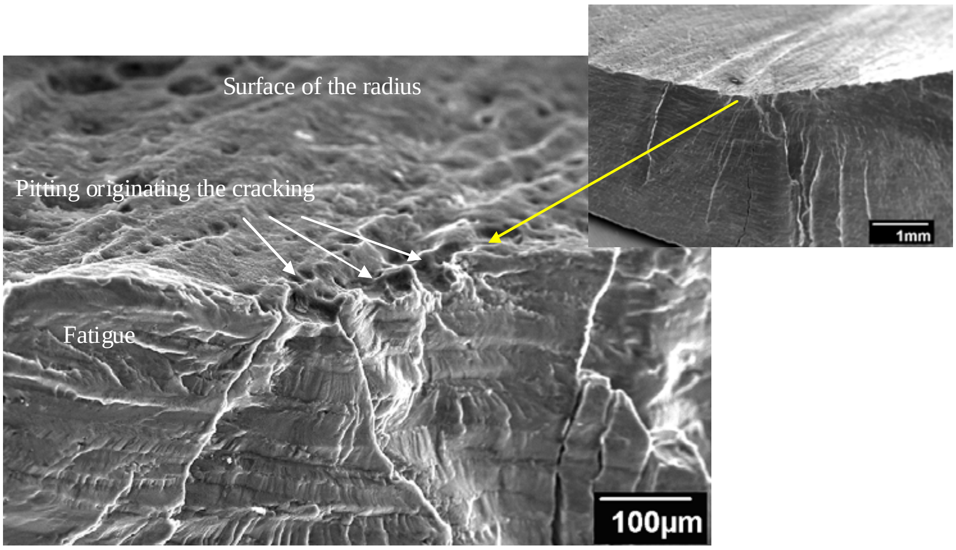

Figure B13: Example of a fatigue crack initiating from etch pits on the surface of a P3C empennage component that had been deoxidised prior to anodising, as part of the production process. The component was an AA7075-T6 extrusion. Note the many other etch pits on the surface.

Example 14: Figure B.14 shows coupon test fatigue cracks growing from defects caused by glass bead peening the aluminium alloy surfaces [B.11]. The first defect is a broad lap, and the second is a cut due to a broken glass bead. For aluminium alloys glass bead peening is preferred to steel shot, which can produce many laps and deep dents in the relatively soft surfaces, and also cause burring-over of corners. Additionally, it is clear from Figure B.14 that laps and cuts due to glass bead peening can initiate fatigue cracks. Hence, it is essential to maintain good control of the entire process, especially the peening intensity and removal of broken beads during recycling.

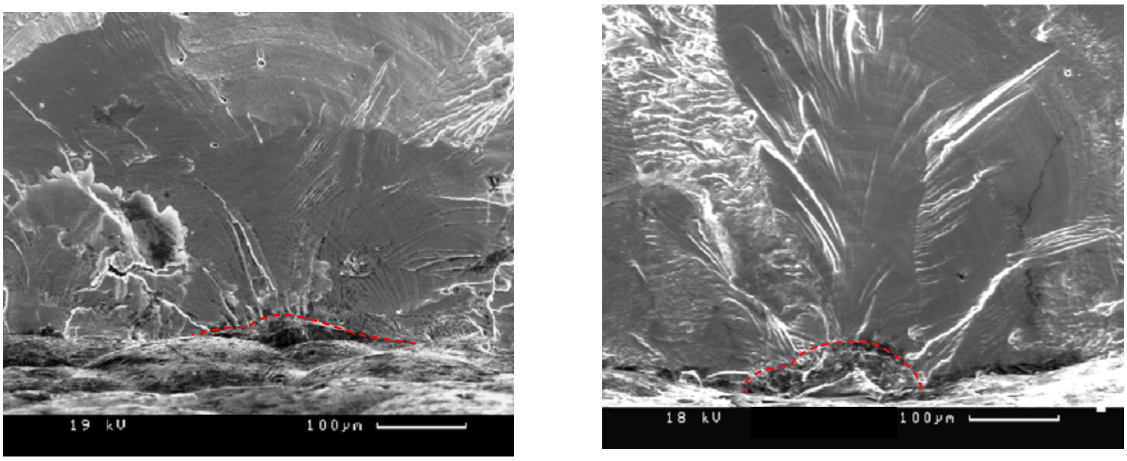

(a) KSIF193

(b) KSIF142

Figure B.14: Two examples of fatigue-initiating discontinuities caused by glass bead peening of test coupons of AA7050-T7451 plate. The red outlines show (a) a broad lap produced by peening, and (b) a deep cut and associated damage caused by impact from a broken glass bead.

B.2.3 Porosity

Porosity is generally rare in wrought aircraft alloys. A notable exception is the aluminium alloy 7050-T7451 thick plate used for heavy-section components like the centre barrels of the F/A-18A/B aircraft. This material is susceptible to mid-thickness porosity, a problem that was not fully appreciated at the time the components were manufactured. This problem led to extensive investigations of thick plate quality, first by the manufacturer [B.12] and later by the DSTO [B.13]. The DSTO work demonstrated that porosity was very occasionally the source for fatigue cracks.

Example 15: Figure B.15 shows an FSFT fatigue crack growing from surface-breaking porosity. This example is also shown as Figure 2B in subsection 3.1 of this report. The pore is large compared to other fatigue-initiating discontinuities. This is because such pores are not crack-like: their physical size is generally much larger than their EPS [B.13].

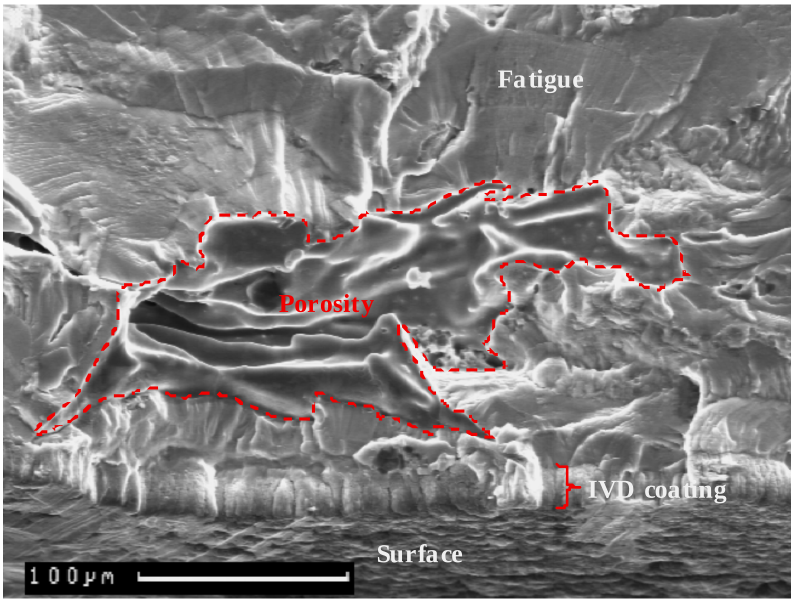

Figure B.15: Example of fatigue growing from many closely spaced origins around a large pore (outlined) in thick plate made from AA7050-T7451.

B.2.4 Constituent particles

Constituent particles are always present in aluminium alloys, and to a lesser extent in aircraft-quality high strength steels. In this subsection–and subsection B.3–we focus on aluminium alloys. These contain several types of constituent particles, which are, however, all hard and brittle intermetallics. The larger particles can crack during bulk processing and also during component machining and finishing. In the latter case they will often be surface-breaking and provide potential sites for crack initiation and lead crack FCG. Three examples are given here.

Example 16: Figure B.16 shows two cracked constituent particles in a 7075-T6 aluminium alloy. The particles cracked during abrasion with 600# SiC paper, which is a relatively mild surface treatment. One of these particles is also shown as Figure 2C in subsection 3.1 of this report.

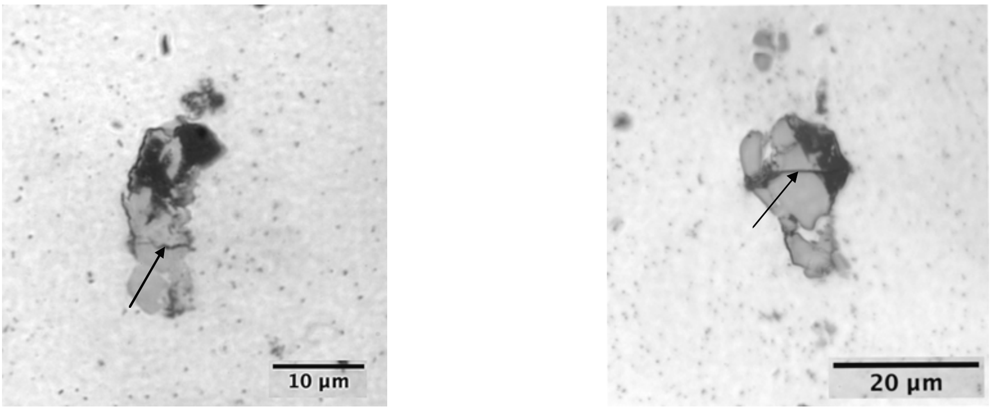

Figure B.16: AA7075-T6 constituent particles that cracked (arrows) during abrasion with 600# SiC paper. The abraded surfaces were electropolished to reveal the cracks.

Example 17: Figure B.17 shows coupon test fatigue cracks growing from several constituent particles in 7050-T7451 aluminium alloy plate [B.7]. Note especially the wide variation in particle shape. This variation is normal, as will be shown in more detail in subsection B.3.2. It must also be mentioned that the importance of fatigue initiation from such particles depends on whether test coupons or actual components are subjected to fatigue. Airframe components will have various production-induced discontinuities; see subsections B.2.2 and B.2.3 that are generally more effective in starting FCG. This is because they are usually larger than cracked or uncracked particles.

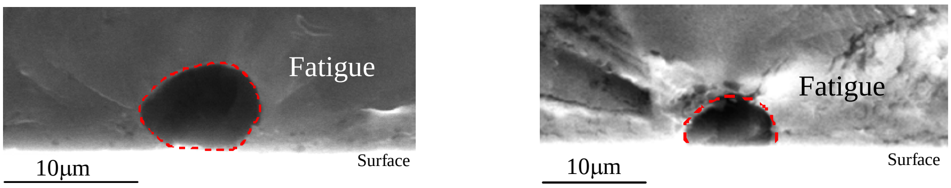
Fatigue
10μm
Surface
Fatigue
10μm
Surface

Oval or circular.

Semi circular or partial oval.

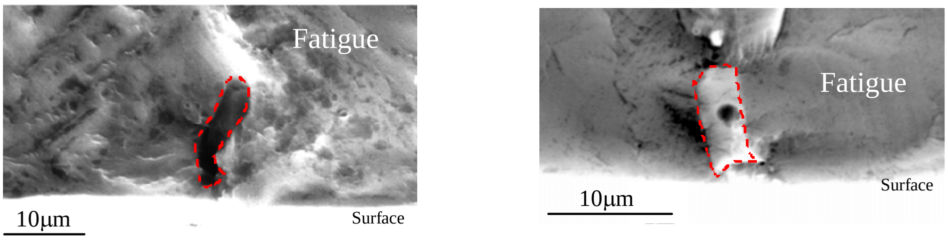
Fatigue
10μm
Surface
Fatigue
10μm
Surface

Long and thin

Square/rectangular

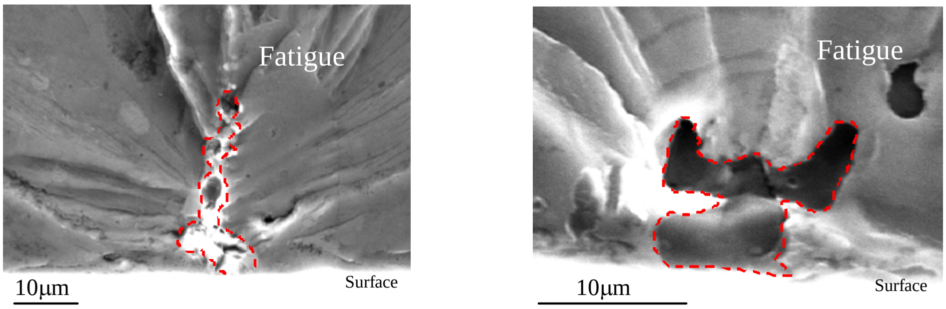
Fatigue
10μm
Surface
Fatigue
10μm
Surface

Thin and deep clusters of inclusions.

‘Moose head’ shaped

Figure B.17: Examples of constituent particles that initiated fatigue cracking in as-machined and reamed holes in AA7050-T7451 fatigue test coupons. The red dashed lines bound the approximate shapes of the particles.

Example 18: Figure B.18 shows an FSFT fatigue crack growing from a large constituent particle at the bottom of a blind fastener hole in a wing main spar [B.14]. The spar was made from AU4SG, which is an aluminium alloy similar to 2014-T6. The fatigue-initiating effectiveness of the particle was most probably increased by its location in a stress-concentrating depression that remained from pilot drilling of the hole.

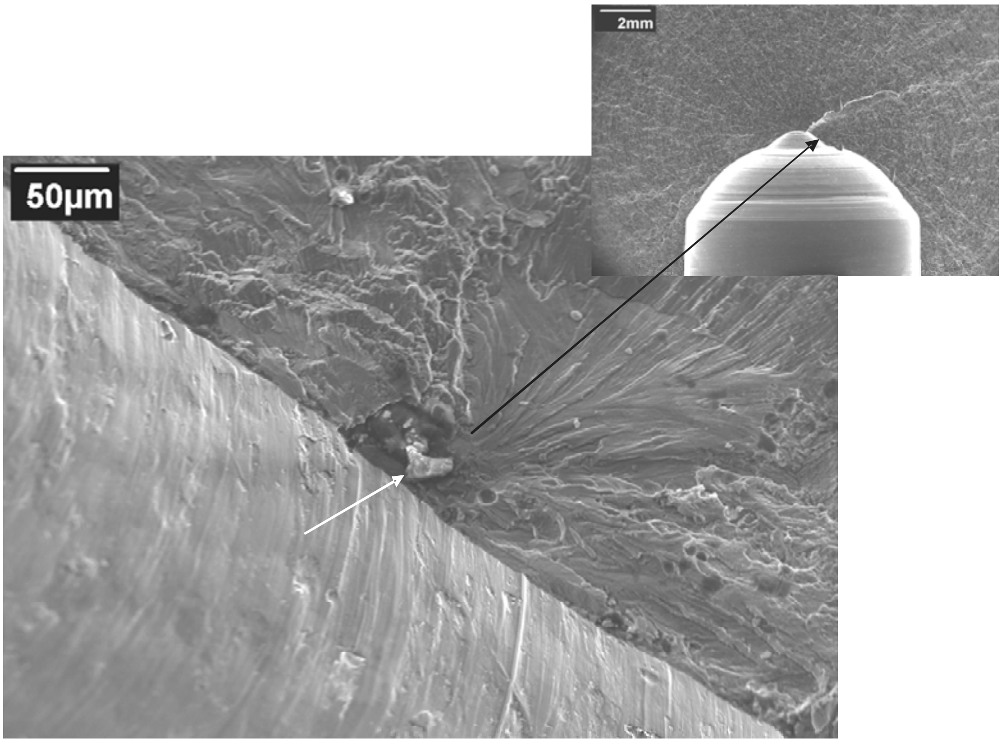

Figure B.18: Example of fatigue cracking from a large constituent particle at the bottom of a blind fastener hole in a wing main spar made from AU4SG aluminium alloy and subjected to an FSFT. Although the hole had a good machined surface, the particle's fatigue-initiating severity was most probably increased by a stress concentration due to the poor shape of the hole tip.

B.3. Fatigue crack initiation in high strength aluminium alloys

In this subsection we shall briefly review the literature on fatigue crack initiation (or nucleation) in high strength aluminium alloys, determined from tests on coupons and specimens with high-quality surface finishes. It should be noted, however, that although the results are interesting from a fundamental viewpoint, their significance for production aircraft components is essentially limited to the effects of large constituent particles. These practical implications of these effects are discussed in subsection B.4.

B.3.1 External or internal initiation

Fatigue cracks in high strength aluminium alloy specimens nearly always initiate at external surfaces. This is the case even in gigacycle fatigue, where internal crack initiation is otherwise the rule for steels, titanium and nickel alloys [B.15]. One exception is when the aluminium alloy surfaces have been shot peened [B.16], as mentioned in subsection 3.2 of this report. See subsection B.3.4 also.

B.3.2 Large constituent particles

Over the last 50–60 years there have been numerous investigations of fatigue crack initiation in high strength aluminium alloys, e.g. [B.17-B.29]. In some of the earlier work there was an understandable tendency to focus on crack initiation and development along slip bands [B.17,B.21], and it was not recognised that fatigue cracks could initiate at large constituent particles unless they were already cracked [B.17]. However, further studies showed that fatigue cracks can nucleate at both cracked and uncracked particles, and that these are the predominant sites of fatigue crack initiation in commercial alloys [B.18–B.20,B.24–B.29]. A recent study of fatigue crack initiation in coupons simulating a critical area in a military aircraft found that *all* the cracks began at cracked particles [B.30].

Figure B.19 gives examples of fatigue crack initiation at cracked and uncracked particles in two commercial alloy specimens, tested under widely different conditions: unnotched *versus* notched, CA loading *versus* flight simulation loading. The particles in Figure B.19a are $FeNiAl_9$ intermetallics, and are characteristic of the alloy, though they need not always be cracked.

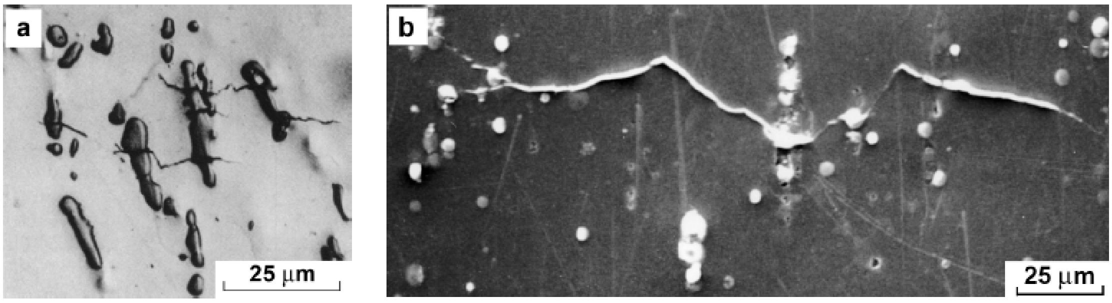

Figure B.19: Fatigue crack initiation at (a) cracked inclusions in a smooth specimen of D.T.D. 5014 aluminium alloy (equivalent to AA2618-T6) tested under CA loading, and (b) uncracked particles in a notched specimen of AA2024-T3 tested under flight-by-flight gust spectrum loading [B.22,B.27].

The sizes of the large particles in Figure B.19 are typical. Quantification of the sizes of constituent particles associated with fatigue crack initiation showed that they often reach depths of 10–20 μm into the specimen surface, but their overall dimensions can be much larger [B.29]. This is illustrated in Figure B.20, which also shows the wide variety of particle shapes, mentioned already in subsection B.2.4 with respect to example 17 and Figure B.17. With respect to composition, $FeNiAl_9$ is specific to iron- and nickel-containing alloys, but there are several kinds of particles that commonly occur in commercial alloys, including $Al_7Cu_2(Fe,Cr)$, $(Fe,Mn)Al_6$, Mg_2Si and Al_2CuMg [B.28,B.29,B.31,B.32]. The recent results mentioned above [B.30] showed that iron-containing particles were nearly always the sites for fatigue cracking.

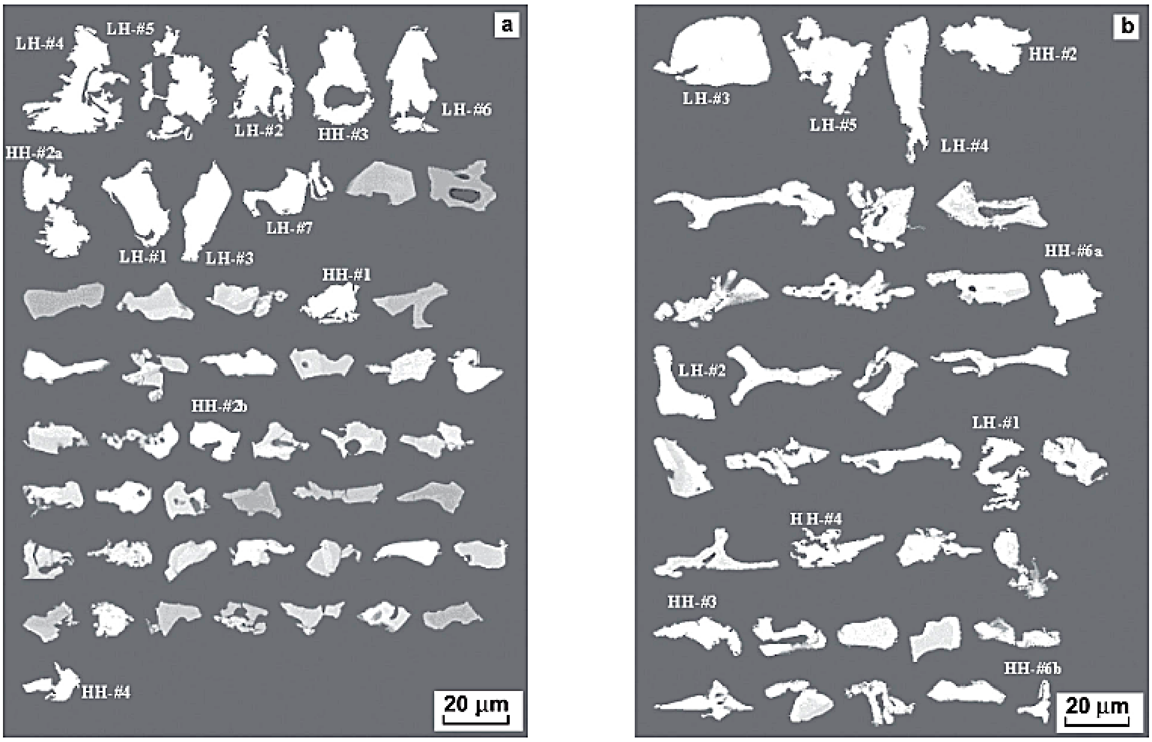

Figure B.20: Comparison between fatigue-initiating large particles and those obtained from metallographic sectioning of the short-transverse planes of (a) thin and (b) thick AA2024-T3 sheet [B.29]. The fatigue-initiating particles are indicated by specimen numbers. The particles are arranged from left to right and from top to bottom in descending order of size (area).

Although large particles are evidently associated with fatigue crack initiation, and there seems to be general agreement that, when the particles are uncracked the cracks initially grow along the particle/matrix interfaces [B.18–B.20,B.22,B.24–B.27,B.29], opinions differ as to whether interfacial debonding is involved [B.20,B.24–B.26,B.29]. Also, it appears that some cracks may start from processing voids between closely-spaced particles [B.25].

Owing to the importance of constituent particles in nucleating fatigue cracks, Grosskreutz and Shaw investigated the effect of reduced particle content on high-cycle reversed-stress notched fatigue of the 2024 aluminium alloy [B.19]. An experimental alloy, X2024-T4, was obtained with more than ten times fewer particles larger than 10 µm. Figure B.21 shows that a relative absence of large particles has a beneficial effect on fatigue compared with commercial alloys, but considering the data scatter the improvement is not large.

B.3.3 Dispersoids and small constituent particles

There are some data on the effects of dispersoids, about 1 µm in size, and small constituent particles in the 0.1–0.2 µm size range, on high-cycle fatigue of high strength aluminium alloys [B.22,B.23,B.33]. Unlike large particles, the presence of these smaller particles can have a beneficial influence on fatigue. This is shown in Figure B.22, which may be compared with Figure B.21.

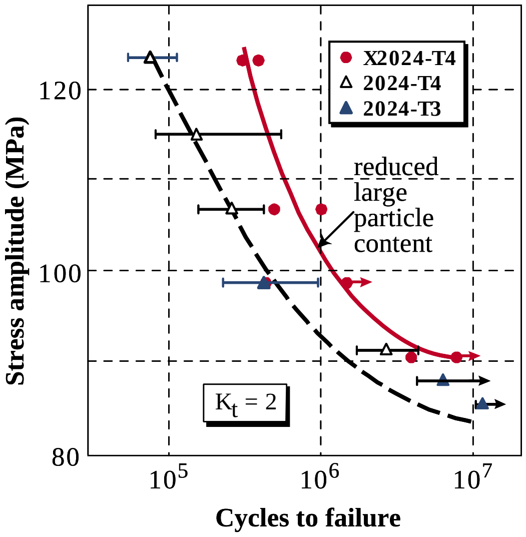

Figure B.21: Effect of reduced large constituent particle (inclusion) content on notched ($K_t = 2$) fatigue of experimental (X) and commercial naturally aged AA2024 [B.19].

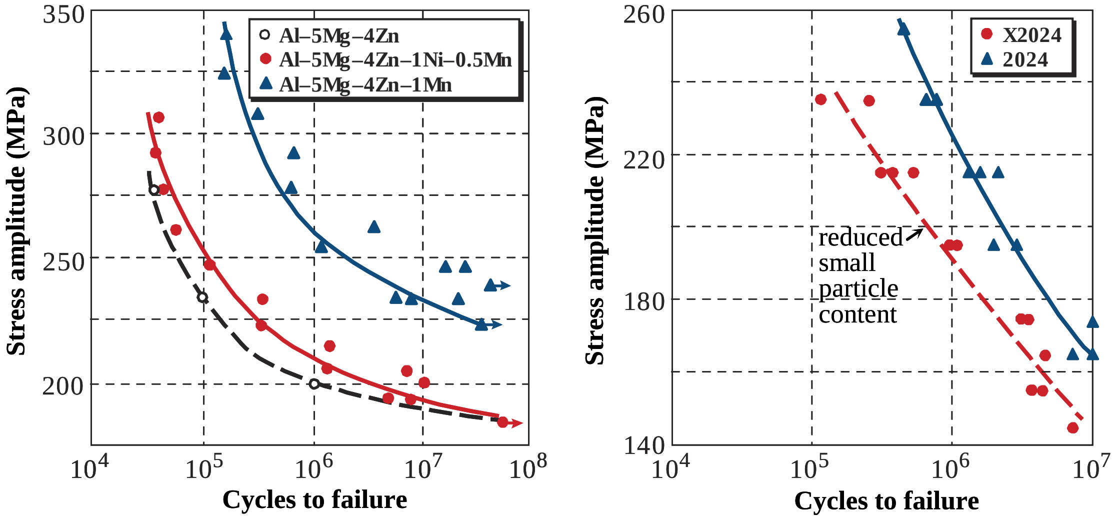

(a) (b)

Figure B.22: Effects of (a) adding Mn- and Ni-containing dispersoids to a ternary peak-aged AlMgZn alloy [B.22,B.33] and (b) reducing the small constituent particle (inclusion) content of naturally aged AA2024 [B.23]. The test specimens were unnotched.

The effects of dispersoids in Figure B.22a may be due partly to preventing recrystallisation and the consequent retention of a fine grain size [B.22,B.33], which would have prevented long dislocation pile-ups along fatigue-induced slip bands, thereby reducing the stress concentrations leading to crack nucleation. However, the dispersoids would also have helped to prevent cyclic slip concentration in narrow bands, as did the small particles in the commercial 2024 aluminium alloy of Figure B.22b [A.2.23].

B.3.4 Internal (subsurface) fatigue initiation

As mentioned in subsection B.3.1, fatigue cracks in high strength aluminium alloys nearly always initiate at external surfaces. There are exceptions, notably when the surfaces have been shot peened. Some unusual examples were also briefly discussed in subsection 3.2 of this report.

Figure B.23 shows subsurface fatigue crack initiation in a shot peened coupon of 7079-T652 aluminium alloy [B.16]. The faceted appearance of the initiation site is typical for vacuum fatigue [B.34]. The crack will have initiated *in vacuo*, most probably by extensive slip band cracking [B.16], although other internal discontinuities, such as large pores and constituent particles can also initiate internal fatigue cracking.

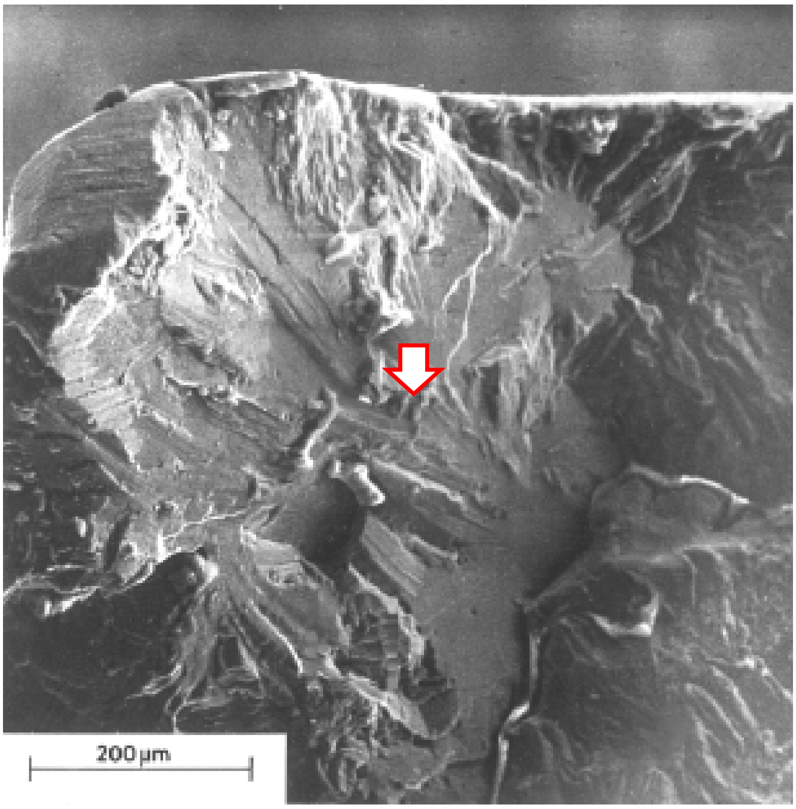

Figure B.23: Subsurface high-cycle fatigue crack initiation in a shot-peened unnotched coupon machined from an AA7079-T652 forging [B.16]. The arrow indicates the approximate location of the fatigue origin.

Several investigations have shown that the high-cycle unnotched fatigue lives of aluminium alloys can be longer *in vacuo* than in air. Some results show life differences for up to $10^7 - 10^8$ cycles [B.34-B.37]. Other data indicate little or no effect at long lives [B.35,B.38–B.40].

More importantly, fatigue cracks can initiate at the same time *in vacuo* and in air [B.34,B.37,B.41] and also (as might be expected) somewhat later [B.38,B.42]. However, even in the latter case it appears that the major environmental effect is on crack growth, which is much slower *in vacuo* than in air [B.34,B.43–B.45]. Note that this was mentioned already in subsection **3.2**.

B.4. References

[B.1] Athiniotis, N., Barter, S.A. and Clark, G. Summary of fatigue cracking in RAAF Macchi MB326H wings, DSTO Technical Report DSTO-TR-0757, Defence Science and Technology Organisation, Melbourne, Australia, 1999.

[B.2] Wanhill, R.J.H., Platenkamp, D.J., Hattenberg, T., Bosch, A.F. and De Haan, P.H. GLARE teardowns from the MegaLiner Barrel (MLB) fatigue test, NLR Technical Publication NLR-TP-2009-068, National Aerospace Laboratory NLR, Amsterdam, the Netherlands, 2009. Also in *ICAF 2009: Bridging the Gap between Theory and Operational Practice*, (editor M.J. Bos), Springer Netherlands, Dordrecht, the Netherlands, pp. 145-167, 2009.

[B.3] Burgess, P.J. Extending the life of the RAAF Macchi jet trainer - selection of the Durability and Damage Tolerance philosophy, Australian Aviation Symposium, Canberra, Australia, 1987.

[B.4] Goldsmith, N.T. and Clark, G. Analysis of wing main spar cracking, *Handbook of Case Histories in Failure Analysis*, (editor K.A. Esakul), ASM International, Metals Park, Ohio, USA, Vol. 1, pp. 9-11, 1992.

[B.5] Huynh, J., Molent, L. and Barter, S.A. Predictions for 7050 aluminium alloy with different stress concentration factors, DSTO Research Report DSTO-RR-0330, Defence Science and Technology Organisation, Melbourne, Australia, 2007.

[B.6] Hartley, D. Australian P-3C empennage fatigue test summary of teardown activities and findings, DSTO Technical Report DSTO-TR-1618, Defence Science and Technology Organisation, Melbourne, Australia, 2004.

[B.7] Huynh, J. and Barter, S.A. Fatigue crack growth in 7050-T7451 aluminium alloy notched coupons, DSTO Technical Report DSTO-TR-1966, Defence Science and Technology Organisation, Melbourne, Australia, 2007.

[B.8] Molent, L., Dixon, B., Barter, S., White, P., Mills, T., Maxfield, K., Swanton, G. and Main, B. Enhanced teardown of ex-service F/A-18A/B/C/D centre fuselages, *ICAF 2009: Bridging the Gap between Theory and Operational Practice*, (editor M.J. Bos), Springer Netherlands, Dordrecht, the Netherlands, pp. 123-142, 2009.

[B.9] Barter, S.A. Investigation of a JAL 747 wing main landing gear trunnion failure, DSTO Contract Report DSTO-CR-2005-0104, Defence Science and Technology Organisation, Melbourne, Australia, 2005.

[B.10] Goldsmith, N.T., Everard, P., Capraro, B. and Byrnes, R. Fractographic examinations of F-111 wing A15-5, DSTO Defence Publication DSTO-DP-00986, Defence Science and Technology Organisation, Melbourne, Australia, 2004.

[B.11] Barter, S.A. Fatigue crack growth in 7050T7451 aluminium alloy thick section plate with a glass bead peened surface simulating some regions of the F/A-18 structure, DSTO Technical Report DSTO-TR-1477, Defence Science and Technology Organisation, Melbourne, Australia, 2003.

[B.12] Magnusen, P.E., Bucci, R.J., Hinkle, A.J., Brockenbrough, J.R. and Konish, H.J. Analysis and prediction of microstructural effects on long-term fatigue performance of an aluminium aerospace alloy, *International Journal of Fatigue*, Vol. 19, Supp. No. 1, pp. S275-S283, 1997.

[B.13] Barter, S.A. Fatigue crack growth in several 7050T7451 aluminium alloy thick section plates with aircraft manufacturer's and laboratory surface finishes representing some regions of the F/A-18 structure, DSTO Technical Report DSTO-TR-1539, Defence Science and Technology Organisation, Melbourne, Australia, 2003.

[B.14] Krieser, R. and Molent, L. (editors). A record of the Australian Mirage wing fatigue test, DSTO Technical Report DSTO-TR-1561, Defence Science and Technology Organisation, Melbourne, Australia, 2004.

[B.15] Bathias, C. Designing components against gigacycle fatigue, *Proceedings of the International Conference on Fatigue in the Very High Cycle Regime*, (editors S.E. Stanzl-Tschegg and H.M. Mayer), Institute of Meteorology and Physics, University of Agricultural Sciences, Vienna, Austria, pp. 97-109, 2001.

[B.16] De Graaf, E.A.B., Wanhill, R.J.H. and De Koning, A.U. Einfluß von Kugelstrahlen und Bohrungsaufweitung auf das Ermüdungsverhalten von AlZnMgCu-Proben, *Aluminium*, Vol. 51, pp. 514-519, 1975.

[B.17] Hunter, M.S. and Fricke, Jr., W.G. Metallographic aspects of fatigue behavior of aluminum, *Proceedings, American Society for Testing and Materials*, Vol. 54, pp. 717-732, 1954.

[B.18] Grosskreutz, J.C. and Shaw, G.G. Mechanisms of fatigue in 1100-0 and 2024-T4 aluminum, Air Force Materials Laboratory Technical Report AFML-TR-65-127, Wright-Patterson Air Force Base, Dayton, Ohio, USA, 1965.

[B.19] Grosskreutz, J.C., Shaw, G.G. and Benson, D.K. The effect of inclusion size and distribution on fatigue of 2024-T4 aluminum, Air Force Materials Laboratory Technical Report AFML-TR-69-121, Wright-Patterson Air Force Base, Dayton, Ohio, USA, 1969.

[B.20] Grosskreutz, J.C. and Shaw, G.G. Critical mechanisms in the development of fatigue cracks in 2024-T4 aluminum, *Fracture 1969*, (editors P.L. Pratt, E.H. Andrews, R.L. Bell, N.E. Frost, R.W. Nichols and E. Smith), Chapman and Hall Ltd., London, UK, pp. 620-629, 1969.

[B.21] Finney, J.M. The relationship between aged structure and the fatigue behaviour of aluminium alloys. Part II: experimental results of aluminium-copper-magnesium alloys, Aeronautical Research Laboratories Structures and Materials Report 325, Melbourne, Australia, 1969.

[B.22] Forsyth, P.J.E. The metallurgical aspects of fatigue and fracture toughness, *Metallurgical Aspects of Fatigue and Fracture Toughness*, AGARD Report No. 610, Advisory Group for Aerospace Research and Development, Neuilly-sur-Seine, France, pp. 1-1 − 1-22, 1973.

[B.23] Lütjering, G., Döker, H. and Munz, D. Microstructure and fatigue behavior of Al-alloys, *Proceedings of the Third International Conference on the Strength of Metals and Alloys*, Institute of Metals, London, UK, pp. 427-431, 1973.

[B.24] Kung, C.Y. and Fine, M.E. Fatigue-crack initiation and microcrack growth in 2024-T4 and 2124-T4 aluminum alloys, *Metallurgical Transactions A*, Vol. 10A, pp. 603-610, 1979.

[B.25] Sigler, D.R., Montpetit, M.C. and Haworth, W.L. Metallography of fatigue crack initiation in an overaged high-strength aluminium alloy, *Metallurgical Transactions A*, Vol. 14A, pp. 931-938, 1983.

[B.26] Newman, Jr., J.C. and Edwards, P.R. *Short-Crack Growth Behaviour in an Aluminum Alloy − An AGARD Cooperative Test Programme*, AGARD Report No. 732, Advisory Group for Aerospace Research and Development, Neuilly-sur-Seine, France, 1988.

[B.27] Wanhill, R.J.H. Damage tolerance engineering property evaluations of aerospace aluminium alloys with emphasis on fatigue crack growth, NLR Technical Publication TP 94177, National Aerospace Laboratory NLR, Amsterdam, the Netherlands, 1995.

[B.28] Barter, S.A., Sharp, P.K., Holden, G. and Clark, G. Initiation and early growth of fatigue cracks in an aerospace aluminium alloy, *Fatigue and Fracture of Engineering Materials and Structures*, Vol. 25, pp. 111-125, 2002.

[B.29] Merati, A. A study of nucleation and fatigue behaviour of an aerospace aluminum alloy 2024-T3, *International Journal of Fatigue*, Vol. 27, pp. 33-44, 2005.

[B.30] Payne, J., Welsh, G., Christ, Jr., R.J., Nardiello, J. and Papazian, J.M. Observations of fatigue crack initiation in 7075-T651, *International Journal of Fatigue*, Vol. 32, pp. 247-255, 2010.

[B.31] Staley, J.T. Microstructure and toughness of high-strength aluminum alloys, *Properties Related to Fracture Toughness,* ASTM STP 605, American Society for Testing and Materials, Philadelphia, Pennsylvania, USA, pp. 71-103, 1976.

[B.32] Kaufman, J.G. Design of aluminum alloys for high toughness and high fatigue strength, *Specialists Meeting on Alloy Design for Fatigue and Fracture Toughness*, AGARD Conference Proceedings No. 185, Advisory Group for Aerospace Research and Development, Neuilly-sur-Seine, France, pp. 2-1 − 2-26, 1976.

[B.33] George, R.W. and Forsyth, P.J.E. The influence of nickel and manganese on the fatigue properties and microstructures of three Al-Mg-Zn alloys, Royal Aircraft Establishment Technical Note No. Met. Phys. 352, Farnborough, UK, 1962.

[B.34] Böhmer, M. Die Beeinflussung des Ermüdungsverhaltens einer Aluminiumlegierung durch den Druck der Luft und ihrer Bestandteile zwischen 760 und 10^{-7} Torr, Deutsche Luft- und Raumfahrt Forschungsbericht 74-19, Deutsche Forschungs- und Versuchsanstalt für Luft- und Raumfahrt Institut für Werkstoff-Forschung, Porz-Wahn, Germany, 1974.

[B.35] Bradshaw, F.J. and Wheeler, C. The effect of environment on fatigue crack growth in aluminium and some aluminium alloys, *Applied Materials Research*, Vol. 5, pp. 112-120, 1966.

[B.36] Shen, H., Podlaseck, S.E. and Kramer, I.R. Effect of vacuum on the fatigue life of aluminum, *Acta Metallurgica*, Vol. 14, pp. 341-345, 1966.

[B.37] Hordon, M.J. Fatigue behavior of aluminum in vacuum, *Acta Metallurgica*, Vol. 14, pp. 1173-1178, 1966.

[B.38] Beitel, G.A. An ultrasonic device for the study of fatigue crack initiation in anodized aluminum alloys, *Corrosion Fatigue: Chemistry, Mechanics and Microstructure*, (editors O.F. Devereux, A.J. McEvily and R.W. Staehle), National Association of Corrosion Engineers, Houston, Texas, USA, pp. 512-517, 1972.

[B.39] Engelmaier, W. Fatigue behavior and crack propagation in 2024-T3 aluminum alloy in ultrahigh vacuum and air, *Transactions of the Metallurgical Society of AIME*, Vol. 242, pp. 1713-1718, 1968.

[B.40] Gough, H.J. and Sopwith, D.G. Atmospheric action as a factor in fatigue of metals, *Journal of the Institute of Metals*, Vol. 49, pp. 93-112, 1932.

[B.41] Wadsworth, N.J. and Hutchings, J. The effect of atmospheric corrosion on metal fatigue, *Philosophical Magazine*, Vol. 3, pp. 1154-1166, 1958.

[B.42] Broom, T. and Nicholson, A. Atmospheric corrosion-fatigue of age-hardened aluminium alloys, *Journal of the Institute of Metals*, Vol. 89, pp. 183-190, 1960-61.

[B.43] Meyn, D.A. The nature of fatigue-crack propagation in air and vacuum for 2024 aluminum, *Transactions of the ASM Quarterly*, Vol. 61, pp. 52-61, 1968.

[B.44] Bradshaw, F.J. and Wheeler, C. The influence of gaseous environment and fatigue frequency on the growth of fatigue cracks in some aluminum alloys, *International Journal of Fracture Mechanics*, Vol. 5, pp. 255-268, 1969.

[B.45] Wanhill, R.J.H. Fractography of fatigue crack propagation in 2024-T3 and 7075-T6 aluminum alloys in air and vacuum, *Metallurgical Transactions A*, Vol. 6A, pp. 1587-1596, 1975.

Appendix C: Lead Crack FCG Estimates

C.1. Introduction

The lead crack fatigue lifing framework has been described in Section 5 of this report. In subsection 5.3 reference was made to examples of estimating the required FCG parameters EPS (equivalent pre-crack size), a_{RS} (critical crack size), and the exponents approximately describing fatigue crack growth between the EPS and a_{RS}. These examples are presented in subsections C.2 and C.3.

The examples refer to the same locations, the fatigue- and fracture-critical web tapers of one of the three bulkheads in the centre barrel (CB) of the F/A-18A/B fuselage. The CB bulkheads are machined from thick 7050-T7451 aluminium alloy plates. Figure C.1 shows an ex-service CB and indicates the two web taper areas and one of the critical locations in the front bulkhead of the three wing carry-though bulkheads. This CB and several others were subjected to post-service full-scale fatigue testing. They provided many of the data used for the lead crack fatigue lifing summarised by Figure 6 in subsection 5.3.

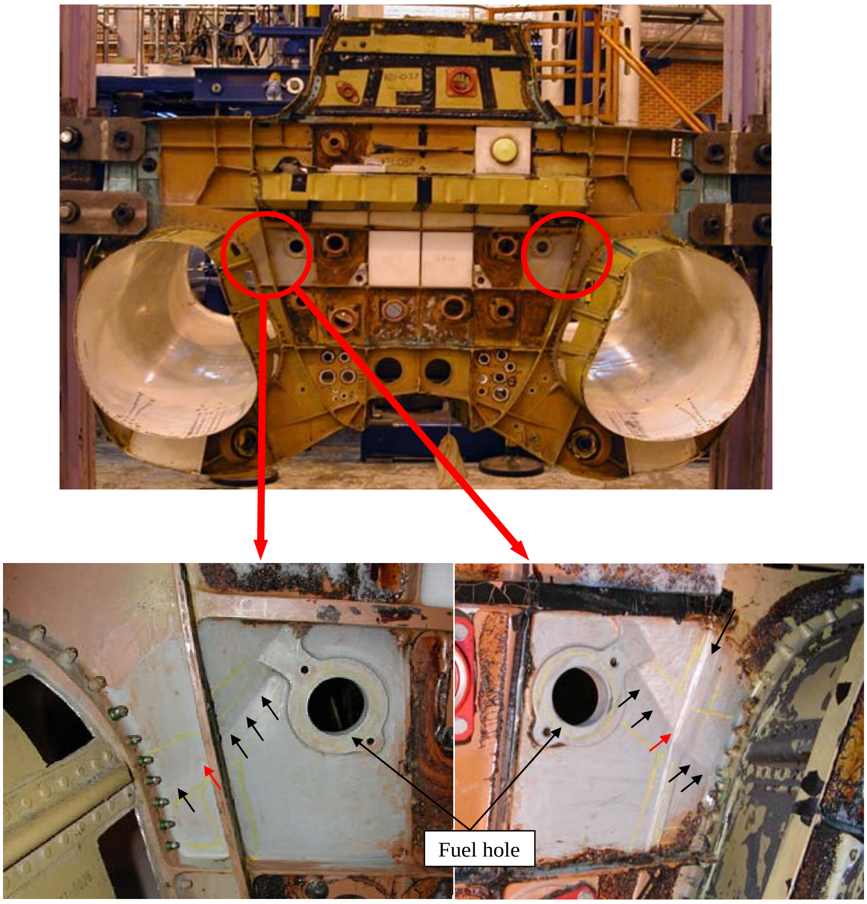

RHS Forward Face

RHS Aft Face

Figure C.1: A centre barrel removed from an F/A-18A showing the two web taper areas (circled) and details of one of them in the front bulkhead of the tested assembly. The small arrows in the lower photographs indicate the fatigue-critical location, with the red arrows pointing to the most critical position along the taper.

C.2. Example of EPS, a_{RS} and lead crack FCG estimates

If there is no information on initial discontinuities, e.g. when a fatigue crack has been blended out, then EPS estimates may be possible by back-extrapolating FCG data for cracks in the same area or location. This scenario applied to a particular CB in which cracks occurred during a FSFT that was part of an international programme [C.1, C.2]. It was also necessary to estimate a_{RS}.

The FSFT was conducted using an as-manufactured CB and a fatigue load history representative of service experience in the web taper areas. During the test the web taper areas were modified in two ways. The RHS web taper was shot peened as part of a series of modifications at 11,375 SFH. Then when cracks were found at 12,656 SFH they were blended out to enable the test to continue. The test ended successfully at the target life of 16,800 SFH.

Post-test NDI detected cracks in the RHS web taper area. These cracks were broken open and the two deepest cracks were selected for QF measurements of FCG. Figure C.2 gives the results and also a lead crack FCG estimate.

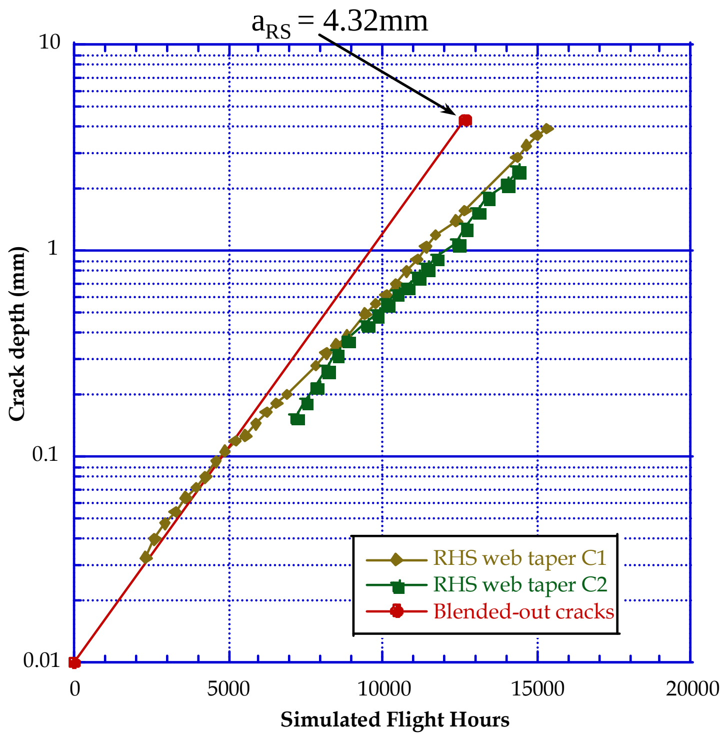

Figure C.2: FCG data and a predicted lead crack FCG plot (FSFT blended-out cracks) for the RHS web taper area of an F/A-18A/B production CB [C.2].

The lead crack estimate was made as follows:

(1) The QF data showed approximately exponential FCG for both cracks. This enabled straightforward back-extrapolation to SFH = 0. Both extrapolations gave an EPS of about 0.01 mm, which was therefore assumed for the blended-out cracks.

(2) The blended-out cracks were assumed to have just penetrated the full thickness of the web taper (4.32 mm at the crack locations) when they were removed. This value was taken as a conservative critical crack size, a_{RS}.

(3) Since the QF data suggested approximately exponential FCG, a lead crack FCG estimate was made by connecting the assumed EPS and a point given by a_{RS} and the SFH at the blending-out time: see the red line in Figure C.2.

Figure C.2 also shows that the lead crack FCG estimate for the blended-out cracks is conservative with respect to the known behaviour of the two nearby cracks. This estimate is therefore consistent with the earlier detection[10] of the blended-out cracks.

Finally, the lead crack FCG estimate was used to estimate a virtual test point for inclusion in steps (4)–(6) of the lead crack fatigue lifing framework described in subsection 5.2 of this report.

C.3. Example of lead crack FCG estimates from multiple cracking

This example comes from an ex-service CB that was subsequently tested without modification of the web taper areas. At the end of the test cracks were detected in both web tapers. However, this example is not as straightforward as the one in subsection C.2. This is because the fatigue load history was designed to test other structural areas and was not fully representative for the web tapers [C.2]. Nevertheless, the test results were useful for lead crack FCG estimates, as will be shown.

The cracked web taper areas were broken open and found to contain multiple fatigue cracks, some of which had coalesced in the RHS web taper. Figures C.3 and C.4 show macroscopic views of fracture surfaces from each web taper. Several cracks were selected for QF measurements of FCG during the test. The reason to do this was that, although the local fatigue load history was not fully representative, it provided easily measured crack front "markers" [C.2,C.3], that would enable determining whether FCG in the web taper areas was approximately exponential.

Figure C.5 presents the QF results. There are three important points to note:

(1) The FCG measurements began at the crack depths reached in service. In other words, a full FCG plot would require the addition of crack growth from initial discontinuities up to the crack depths when testing commenced. This is not necessary at this stage of the estimation procedure.

---

[10] It is important to distinguish between the *detection* and *occurrence* of cracks. Although the nearby cracks were found at the end of testing, the QF data in Figure C.2 suggest that these cracks grew almost from the start of the FSFT. This would also be the case for the lead cracks, which by definition grew faster and were therefore detected during testing

(2) Most of the cracks showed approximately exponential FCG, although some deviations occurred beyond crack depths ≥ 0.1 mm, notably for cracks in the RHS web taper. Deviations were caused by the cessation of loading to a nearby bulkhead which then parasitically lowered the load in the RHS of the bulkhead being examined here. As such these deviations were due to geometrical influences and load shedding. See subsections A.3 and A.4 for discussions on these topics.

(3) The lead cracks were CB12 LHS C1 and CB12 RHS C1.

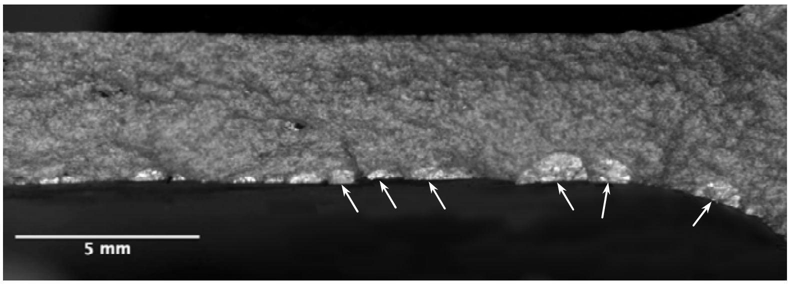

Figure C.3: Fracture surface of the broken-open fatigue cracked area in the LHS web taper from an ex-service CB tested until cracking was detected. Some of the exposed fatigue cracks are marked.

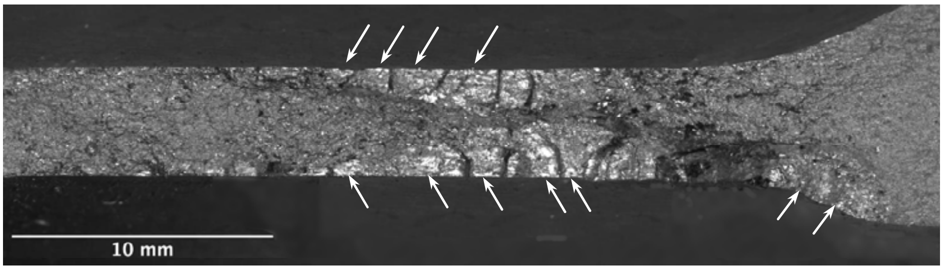

Figure C.4: Fracture surface of the broken-open fatigue cracked area in the RHS web taper from an ex-service CB tested until cracking was detected. Some of the exposed fatigue cracks are marked.

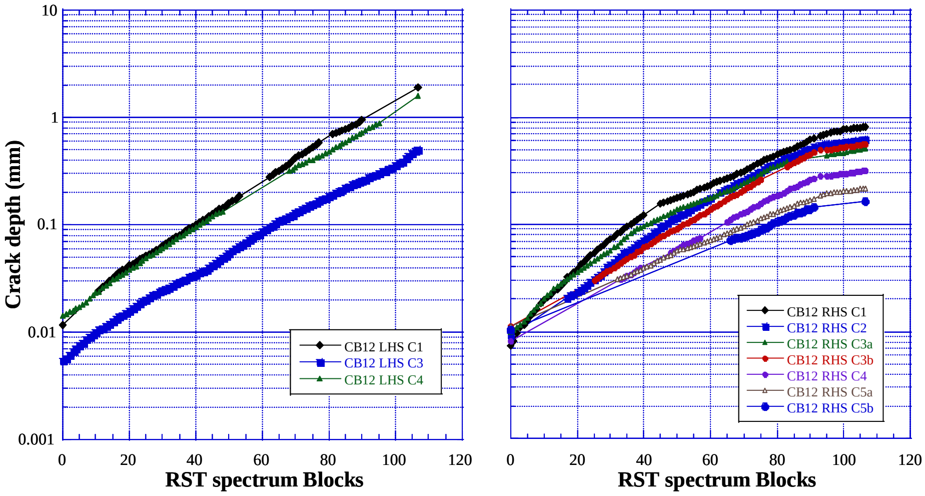

Figure C.5: FCG test data for selected cracks from the web taper areas of an F/A-18A/B ex-service CB. The CB was tested with an RST spectrum developed principally to test other structural areas [C.2].

In the light of the results shown in Figure C.5 it was considered reasonable to assume exponential FCG for the in-service cracks in the web taper areas. The following additional steps were taken to obtain the lead crack FCG estimates for the in-service grown cracks:

(4) Determination of the EPS values for the initial discontinuities of the selected cracks [C.2]– in this case the measured depths of the initiating discontinuities were used.

(5) Connection of the EPS values to the crack depths reached in service, using a log crack depth *versus* flight hours plot, and extrapolation to the critical crack size to determine which cracks would give the shortest lives. These were designated the lead cracks.

Figure C.6 gives the results of steps (4) and (5). Note that the lead cracks were CB12 LHS C2 and CB12 RHS C1, as in Figure C.5, but that this was not at first the case for either CB12 LHS C2 or CB12 RHS C1. A similar result was described at the end of Section 2 of this report.

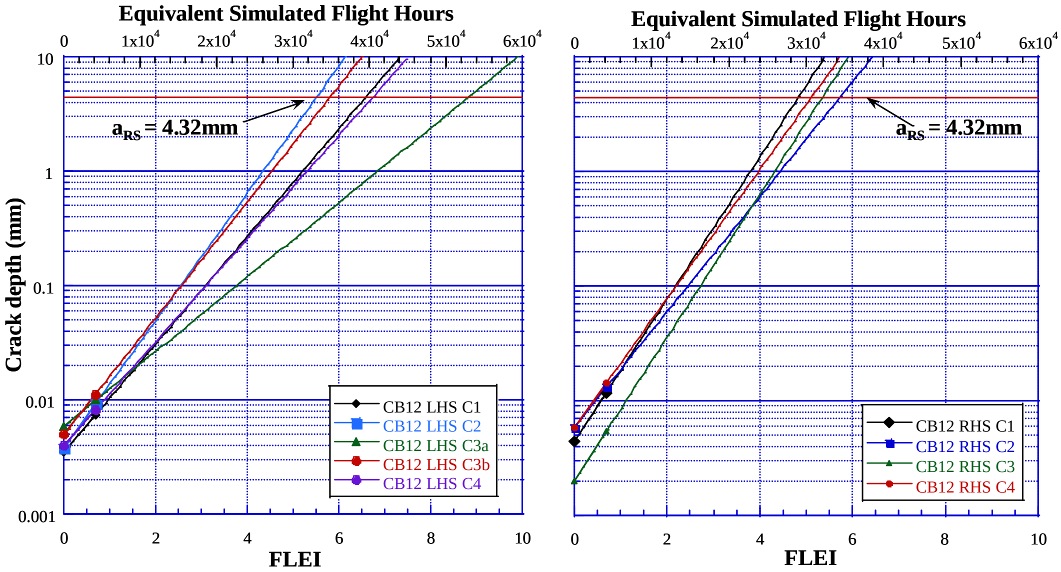

Figure C.6: In-service FCG data points and conservatively-predicted FCG plots for the cracks whose test data are shown in Figure C.5. The equivalent lives in terms of the FSFT are given at the tops of the graphs.

Finally, the CB12 LHS C2 and CB12 RHS C1 lead crack FCG estimates were used to estimate virtual test points for inclusion in steps (4)—(6) of the lead crack fatigue lifing framework described in subsection 5.2 of this report.

Also illustrated in Figure C.6 is that for a similar FLEI and depth of a service crack, extrapolating from a smaller EPS will lead to a more conservative estimate of life than a larger EPS, see [C.4].

C.4. References

[C.1] Simpson, D.L., Landry, N., Roussel, J., Molent, L., Graham, A.D. and Schmidt. N. The Canadian and Australian F/A-18 international follow-on structural test project, *ICAS Proceedings 2002: 23rd Congress of the International Council of the Aeronautical Sciences*, (editor I. Grant) Toronto, Canada, 2002.

[C.2] Barter, S., Molent, L. and Robertson, L. Using in-service F/A-18 A / B aircraft fatigue cracking as disclosed by teardown to refine fleet life limits. *Proceedings of the 2009 USAF Structural Integrity Program (ASIP) Conference*, Jacksonville, Florida, USA, 30 November - 2 December. 2009.

[C.3] Barter, S.A., Molent, L. and Wanhill, R.J.H. Marker loads for quantitative fractography of fatigue cracks in aerospace alloys, *ICAF 2009: Bridging the Gap between Theory and Operational Practice*, (editor M.J. Bos), Springer Netherlands, Dordrecht, the Netherlands, pp. 15-54, 2009.

[C.4] Molent, L., Singh, R. and Woolsey, J. A method for evaluation of in-service fatigue cracks, *Engineering Failure Analysis*, Vol. 12, pp. 13-24, 2005.

DEFENCE SCIENCE AND TECHNOLOGY ORGANISATION
DOCUMENT CONTROL DATA

1. PRIVACY MARKING/CAVEAT (OF DOCUMENT)

2. TITLE	3. SECURITY CLASSIFICATION (FOR UNCLASSIFIED REPORTS THAT ARE LIMITED RELEASE USE (L) NEXT TO DOCUMENT CLASSIFICATION)
The Lead Crack Fatigue Lifing Framework	Document (U) Title (U) Abstract (U)

4. AUTHOR(S)	5. CORPORATE AUTHOR
L. Molent, S.A. Barter and R.J.H. Wanhill	DSTO Defence Science and Technology Organisation 506 Lorimer St Fishermans Bend Victoria 3207 Australia

6a. DSTO NUMBER	6b. AR NUMBER	6c. TYPE OF REPORT	7. DOCUMENT DATE
DSTO-RR-0353	AR-014-747	Research Report	April 2010

8. FILE NUMBER	9. TASK NUMBER	10. TASK SPONSOR	11. NO. OF PAGES	12. NO. OF REFERENCES
2010/10220014	07/048	DGTA	58	101

13. URL on the World Wide Web	14. RELEASE AUTHORITY
http://www.dsto.defence.gov.au/corporate/reports/DSTO-RR-0353.pdf	Chief, Air Vehicles Division

15. SECONDARY RELEASE STATEMENT OF THIS DOCUMENT

Approved for public release

OVERSEAS ENQUIRIES OUTSIDE STATED LIMITATIONS SHOULD BE REFERRED THROUGH DOCUMENT EXCHANGE, PO BOX 1500, EDINBURGH, SA 5111

16. DELIBERATE ANNOUNCEMENT

No Limitations

17. CITATION IN OTHER DOCUMENTS Yes

18. DSTO RESEARCH LIBRARY THESAURUS http://web-vic.dsto.defence.gov.au/workareas/library/resources/dsto_thesaurus.shtml

Fatigue Tests; Fatigue Loads; Cracking (Fracturing); Crack Propagation; Fatigue Lifing

19. ABSTRACT

A fatigue lifing framework using a lead crack concept has been developed by the DSTO for metallic primary airframe components. The framework is based on years of detailed inspection and analysis of fatigue cracks in many specimens and airframe components, and is an important additional tool for determining aircraft component fatigue lives in the Royal Australian Air Force (RAAF) fleet. Like the original Damage Tolerance (DT) concept developed by the United States Air Force (USAF), this framework assumes that fatigue cracking begins as soon as an aircraft enters service. However, there are major and fundamental differences. Instead of assuming initial crack sizes and deriving early crack growth behaviour from back-extrapolation of growth data for long cracks, the DSTO framework uses data for real cracks growing from small discontinuities inherent to the material and the production of the component. Furthermore, these data, particularly for lead cracks, are characterized by exponential crack growth behaviour. Because of this common characteristic, the DSTO framework can use lead crack growth data to provide reasonable (i.e. not overly conservative) lower-bound estimates of typical crack growth lives of components, starting from small natural discontinuities and continuing up to crack sizes that just meet the residual strength requirements. Scatter factors based on engineering judgement are then applied to these estimates to determine the maximum allowable service life (safe life limit).